

Counterexamples to Moffatt's statements on vortex knots

Oleg Bogoyavlenskij

Department of Mathematics and Statistics, Queen's University, Kingston, Ontario, Canada K7L 3N6

(Received 1 August 2016; revised manuscript received 12 January 2017; published xxxxxx)

One of the well-known problems of hydrodynamics is studied: the problem of classification of vortex knots for ideal fluid flows. In the literature there are known Moffatt statements that all torus knots $K_{m,n}$ for all rational numbers m/n ($0 < m/n < \infty$) are realized as vortex knots for each one of the considered axisymmetric fluid flows. We prove that actually such a uniformity does not exist because it does not correspond to the facts. Namely, we derive a complete classification of all vortex knots realized for the fluid flows studied by Moffatt and demonstrate that the real structure of vortex knots is much more rich because the sets of mutually nonisotopic vortex knots realized for different axisymmetric fluid flows are all different. An exact formula for the limit of the hydrodynamic safety factor q_h at a vortex axis is derived for arbitrary axisymmetric fluid equilibria. Another exact formula is obtained for the limit of the magnetohydrodynamics safety factor q at a magnetic axis for the general axisymmetric plasma equilibria.

DOI: [10.1103/PhysRevE.00.003100](https://doi.org/10.1103/PhysRevE.00.003100)

I. INTRODUCTION

Euler equations of the dynamics of an ideal incompressible fluid with a constant density ρ have the form

$$\frac{\partial \mathbf{V}}{\partial t} + (\mathbf{V} \cdot \text{grad})\mathbf{V} = -\text{grad}\left(\frac{p}{\rho} + \Phi\right), \quad \text{div } \mathbf{V} = 0. \quad (1.1)$$

Here $\mathbf{V}(t, \mathbf{x})$ is the fluid velocity vector field, $p(t, \mathbf{x})$ the pressure, and Φ the gravitational potential. As known, the vortex field $\text{curl } \mathbf{V}$ is transformed in time by the flow diffeomorphisms (or “is frozen in the flow” [1]) and therefore any knot formed by a closed vortex line at a time t is transformed by the flow into an isotopic knot.

Since Kelvin's works there exists the problem of classification of all mutually nonisotopic vortex knots for concrete solutions to Euler equations (1.1). For the steady axisymmetric fluid flows, this problem was studied by Moffatt in [2–4], where he claimed that all torus knots $K_{m,n}$ for all rational numbers m/n ($0 < m/n < +\infty$) are realized as vortex knots for all considered flows. We show in this paper that such a uniformity actually does not exist and that the families of mutually nonisotopic vortex knots realized for different axisymmetric fluid flows are in general different.

Axisymmetric steady fluid flows have velocity vector fields

$$\mathbf{V}(r, z) = -\frac{1}{r} \frac{\partial \psi}{\partial z} \hat{\mathbf{e}}_r + \frac{1}{r} \frac{\partial \psi}{\partial r} \hat{\mathbf{e}}_z + \frac{w(r, z)}{r} \hat{\mathbf{e}}_\varphi, \quad (1.2)$$

where $\psi(r, z)$ is the Stokes stream function and $\hat{\mathbf{e}}_r$, $\hat{\mathbf{e}}_z$, and $\hat{\mathbf{e}}_\varphi$ are the unit ords in the cylindrical coordinates r , z , and φ . The steady axisymmetric Euler equations (1.1) are reduced to the Grad-Shafranov equation

$$\psi_{rr} - \frac{1}{r} \psi_r + \psi_{zz} = r^2 \frac{dH}{d\psi} - C \frac{dC}{d\psi}, \quad (1.3)$$

where $H(\psi)$ and $C(\psi)$ are arbitrary smooth functions connected with the vector field \mathbf{V} [Eq. (1.2)] and pressure p by the relations [1]

$$\frac{p}{\rho} + \Phi + \frac{1}{2} |\mathbf{V}|^2 = H(\psi), \quad w(r, z) = C(\psi). \quad (1.4)$$

The Grad-Shafranov equation (1.3) was first derived for the plasma equilibria

$$\text{curl } \mathbf{B} \times \mathbf{B} = \text{grad}(\mu p + \rho \mu \Phi), \quad \text{div } \mathbf{B} = 0, \quad (1.5)$$

where $\mathbf{B}(\mathbf{x})$ is the magnetic field and μ the magnetic permeability. The hydrodynamics equilibrium equations

$$\text{curl } \mathbf{V} \times \mathbf{V} = -\text{grad}(p/\rho + \rho \mu \Phi + |\mathbf{V}|^2/2), \quad \text{div } \mathbf{V} = 0 \quad (1.6)$$

and Eqs. (1.5) are equivalent [5].

Kruskal and Kulsrud [6] proved for Eqs. (1.5) that surfaces $p(\mathbf{x}) = \text{const}$ “by $\mathbf{B} \cdot \nabla p = 0$ are ‘magnetic surfaces’, in the sense that they are made up of lines of magnetic force, and simultaneously by $\mathbf{j} \cdot \nabla p = 0$ they are ‘current surfaces’. If such a surface lies in a bounded volume of space and has no edges and if either \mathbf{B} or \mathbf{j} nowhere vanishes on it, then by a well-known theorem [7] it must be a toroid (by which we mean a topological torus) or a Klein bottle. The latter, however is not realizable in physical space”.

Newcomb [8] stated that “it is easy to verify that the lines of force on a pressure surface are closed if and only if $\iota(P)/2\pi$ is rational; if it is irrational, the lines of force cover the surface ergodically”. Here $\iota(P)$ is the rotational transform connected with the safety factor $q(P)$ [9] by the relation $q(P) = 2\pi/\iota(P)$. The safety factor q and the rotational transform $\iota = 2\pi/q$ are connected with stability of the plasma equilibria [9].

The analogous results for the equivalent equations (1.6) were published by Arnold in [10,11], where he added to [6,8] a statement that if a Bernoulli surface M intersects the boundary of the invariant domain D then M has “coordinates of the ring” and “all streamlines on M are closed”. The results of [6,8] imply that for the plasma equilibrium equations (1.5) [and hence for the equivalent hydrodynamics equations (1.6)] all magnetic field knots (and correspondingly all vortex knots) are torus knots $K_{m,n}$ defined by the rational values m/n of the safety factor $q(P)$. Therefore, to classify the magnetic knots in magnetohydrodynamics (MHD) and vortex knots in steady hydrodynamics it is necessary to know the ranges of the corresponding safety factors.

78 For the fluid velocity field $\mathbf{V}(\mathbf{x})$ [Eq. (1.2)] its vortex
79 field is

$$\text{curl } \mathbf{V} = -\frac{C(\psi)_z}{r} \hat{\mathbf{e}}_r + \frac{C(\psi)_r}{r} \hat{\mathbf{e}}_z - \frac{1}{r} \left(\psi_{rr} - \frac{1}{r} \psi_r + \psi_{zz} \right) \hat{\mathbf{e}}_\varphi. \quad (1.7)$$

80 The surfaces $\psi(r, z) = \text{const}$ are invariant for both flows $\mathbf{V}(\mathbf{x})$
81 [Eq. (1.2)] and $\text{curl } \mathbf{V}(\mathbf{x})$ [Eq. (1.7)]. The smooth axisymmetric
82 surfaces $\psi(r, z) = \text{const}$ are either tori $\mathbb{T}_\psi^2 = C_\psi \times \mathbb{S}^1 \subset \mathbb{R}^3$,
83 or spheres \mathbb{S}_ψ^2 or cylinders $\mathbb{C}_\psi^2 = R_\psi \times \mathbb{S}^1$. Here the closed
84 curves C_ψ and infinite lines R_ψ are purely poloidal, lie in the
85 plane (r, z) , and satisfy equation $\psi(r, z) = \text{const}$. The circle \mathbb{S}^1
86 corresponds to the angular coordinate $0 \leq \varphi \leq 2\pi$ and is z
87 axisymmetric.

88 If a surface $\psi(r, z) = \text{const}$ is a torus $\mathbb{T}_\psi^2 = C_\psi \times \mathbb{S}^1$ then
89 the fluid streamlines and vortex lines on the \mathbb{T}_ψ^2 are either
90 infinite helical curves or closed curves. Moffatt's definition
91 of the pitch (see [2], pp. 128–129) is as follows: “If any
92 one vortex line is followed in the direction of increasing φ
93 the value of z on that line varies periodically; the *pitch* p of the
94 vortex line may conveniently be defined as twice the increase
95 of φ , between successive zeros of z ”. The Moffatt definition is
96 not applicable to the vortex lines on tori \mathbb{T}_ψ^2 that are located in
97 domains $z > 0$ or $z < 0$ because there are no successive zeros
98 of z on those vortex lines. The definition is applicable only if
99 the poloidal curves C_ψ (and hence the tori $\mathbb{T}_\psi^2 = C_\psi \times \mathbb{S}^1$) are
100 invariant under the reflection $z \rightarrow -z$, because only then the
101 words “twice” and “successive zeros of z ” become meaningful.
102 This is true for the special solutions considered in [2], but not
103 for the general case. Therefore, we will use another definition
104 of the pitch.

105 *Definition 1.* The pitch $p(\psi)$ of a vortex line on a torus
106 $\mathbb{T}_\psi^2 = C_\psi \times \mathbb{S}^1$ is the change of the angle φ along the vortex
107 line when its poloidal projection makes one complete turn
108 around the closed curve C_ψ . The formula for the pitch is

$$p(\psi) = \int_0^{t(\psi)} \frac{d\varphi}{dt} dt, \quad (1.8)$$

109 where the integral is taken along the $\text{curl } \mathbf{V}$ line and $t(\psi)$ is the
110 period of its poloidal projection C_ψ . The hydrodynamic safety
111 factor $q_h(\psi)$ is

$$q_h(\psi) = \frac{p(\psi)}{2\pi}. \quad (1.9)$$

112 Note that the pitch function $p(\psi)$ [Eq. (1.8)] is positive if
113 the clockwise rotation along the curve C_ψ is accompanied by
114 the increase of the total angle φ and $p(\psi)$ is negative if the
115 total change of angle φ is negative. Definition 1 conforms to
116 Moffatt's definition [2] when the curve C_ψ is invariant under
117 the reflection $z \rightarrow -z$. Suppose the pitch is $p(\psi) = 2\pi m/n$,
118 where m and n are integers [i.e., the safety factor $q_h(\psi) =$
119 m/n]. Then, after n complete turns of the vortex line around the
120 poloidal circle C_ψ , the angle φ is changed for $np(\psi) = 2\pi m$.
121 Hence the vortex line is a closed curve because its end and
122 starting points coincide. In other words, the vortex line is a
123 torus knot $K_{m,n} \subset \mathbb{R}^3$.

124 If a closed magnetic field \mathbf{B} line on a torus \mathbb{T}_ψ^2 makes m turns
125 the long way \mathbb{S}^1 around and n turns the short way C_ψ around
126 then its safety factor q is, as defined in [9,12], $q = m/n$.

Definition 2. The safety factor $q(\psi)$ of a magnetic field \mathbf{B}
127 line on a torus $\mathbb{T}_\psi^2 = C_\psi \times \mathbb{S}^1$ is the divided by 2π change of
128 the azimuthal angle φ along the magnetic field line when its
129 poloidal projection makes one complete turn around the closed
130 curve C_ψ . The corresponding formula is
131

$$q(\psi) = \frac{1}{2\pi} \int_0^{t(\psi)} \frac{d\varphi}{dt} dt. \quad (1.10)$$

132 Here the integral is taken along the magnetic field \mathbf{B} line
133 on the torus \mathbb{T}_ψ^2 and $t(\psi)$ is the period of its poloidal
134 projection C_ψ .

135 For the closed magnetic field \mathbf{B} -line definition (1.10)
136 conforms to the definition in [9,12]. For the same ψ function
137 $\psi(r, z)$, the two safety factors $q_h(\psi)$ and $q(\psi)$ are qualitatively
138 different because they are defined correspondingly for the
139 $\text{curl } \mathbf{V}$ in (1.6) and the magnetic field \mathbf{B} in (1.5) that is
140 analogous to the fluid velocity \mathbf{V} in the equivalent equations
141 (1.6). For example, when $q_h(\psi)$ [Eq. (1.9)] is a rational number
142 m/n and hence the corresponding vortex line is a torus knot
143 $K_{m,n}$, the MHD safety factor $q(\psi)$ [Eq. (1.10)] in general is
144 an irrational number and the corresponding magnetic field \mathbf{B}
145 line is an infinite curve that is dense on the invariant torus
146 $\mathbb{T}_\psi^2 = C_\psi \times \mathbb{S}^1$ and vice versa. Neither the pitch p nor the
147 safety factor q_h is defined for the vortex lines belonging
148 to invariant spheres \mathbb{S}_ψ^2 or cylinders $\mathbb{C}_\psi^2 = R_\psi \times \mathbb{S}^1$ where
149 $\psi(r, z) = \text{const}$.

150 In Sec. II we derive for the general solutions to the Grad-
151 Shafranov equation (1.3) the exact formula for the limit of the
152 hydrodynamic safety factor $q_h(\psi)$ [Eq. (1.9)] at the vortex axis
153 $\mathbb{S}_{\psi_m}^1$ ($r = r_m, z = z_m, 0 \leq \varphi \leq 2\pi$), $\psi_m = \psi(r_m, z_m)$:

$$q_h(\psi_m) = -\frac{\Delta\psi(a_m)}{r_m C'(\psi_m) \sqrt{\mathcal{H}(a_m)}}. \quad (1.11)$$

154 Here Δ is the Laplace operator and $\mathcal{H}(a_m) =$
155 $\psi_{rr}(a_m)\psi_{zz}(a_m) - \psi_{rz}^2(a_m) \geq 0$ is the Hessian of the
156 function $\psi(r, z)$ at the point $a_m = (r_m, z_m)$.

157 *Remark 1.* Formulas (1.9) and (1.11) prove that Moffatt's
158 statements of [2–4], that at the vortex axis $\mathbb{S}_{\psi_m}^1$ the limit of
159 the pitch $p(\psi_m)$ is always equal to infinity (or twist 0), can be
160 true only for the degenerate solutions to the Grad-Shafranov
161 equation (1.3) for which either $C'(\psi_m) = 0$ or $\mathcal{H}(a_m) = 0$.
162 For the solutions studied by Moffatt $C'(\psi_m) = \alpha \neq 0$ and
163 $\mathcal{H}(a_m) \neq 0$.

164 In Sec. III we derive for the general axisymmetric plasma
165 equilibria (1.5) the exact formula for the limit of the MHD
166 safety factor $q(\psi)$ [Eq. (1.10)] at a magnetic axis

$$q(\psi_m) = \frac{C(\psi_m)}{r_m \sqrt{\mathcal{H}(a_m)}}. \quad (1.12)$$

167 The formulas (1.11) and (1.12) are evidently different. This
168 reflects the fact that for the same stream (or flux) function
169 $\psi(r, z)$ the topological properties of the vortex field $\text{curl } \mathbf{V}(\mathbf{x})$
170 and magnetic field $\mathbf{B}(\mathbf{x})$ are essentially different.

171 There are two cases for which Eq. (1.3) becomes linear:

$$H(\psi) = H_1 + c^2 \psi^2, \quad C(\psi) = \alpha \psi, \quad (1.13)$$

$$H(\psi) = \lambda \psi, \quad C(\psi) = \alpha \psi. \quad (1.14)$$

Exact solutions for the case (1.13) that are global plasma equilibria modeling astrophysical jets are presented in [13–15], where also extensive literature for the case (1.13) is quoted.

In Secs. IV–VII we study solutions to the Grad-Shafranov equation (1.3) satisfying the conditions (1.14):

$$\psi_{rr} - \frac{1}{r}\psi_r + \psi_{zz} = \alpha^2(\xi r^2 - \psi), \quad \xi = \lambda/\alpha^2. \quad (1.15)$$

Substituting formulas (1.14) and (1.15) into Eq. (1.7), we find

$$\text{curl } \mathbf{V} = \alpha \mathbf{V} - \alpha^2 \xi r \hat{\mathbf{e}}_\varphi. \quad (1.16)$$

Hence vector fields $\mathbf{V}(r, z)$ [Eqs. (1.2) and (1.15)] for $\xi \neq 0$ are not Beltrami flows. They satisfy the Beltrami equation

$$\text{curl } \mathbf{V}_0 = \alpha \mathbf{V}_0 \quad (1.17)$$

only for $\xi = 0$. Therefore, the parameter ξ has the following physical meaning: It defines the deviation of the fluid flow $\mathbf{V}(r, z)$ [Eqs. (1.2) and (1.15)] from the Beltrami flow $\mathbf{V}_0(r, z)$ [Eq. (1.17)].

We study the fluid flows $\mathbf{V}_\xi(r, z)$ [Eqs. (1.2) and (1.15)] that have the Stokes function

$$\psi(r, z) = r^2[\xi - G_2(\alpha R)], \quad R = \sqrt{r^2 + z^2}, \quad (1.18)$$

where

$$G_2(u) = u^{-2}(\cos u - u^{-1} \sin u). \quad (1.19)$$

The parameters $\alpha \neq 0$ and ξ take all real values from $(-\infty, \infty)$. The parameter $\alpha \neq 0$ in view of (1.18) specifies the scaling of the fluid equilibria $\mathbf{V}_\xi(r, z)$ and its sign indicates the direction of fluid rotation $[\mathbf{V}_\xi(r, z)]_\varphi = \alpha r^{-1} \psi$ [Eqs. (1.2) and (1.14)]. Substituting the Stokes function (1.18) and $w(r, z) = \alpha \psi$ into Eq. (1.2), we get the fluid velocity field

$$\mathbf{V}_\xi(r, z) = \alpha^2 r z G_3(\alpha R) \hat{\mathbf{e}}_r + \{2[\xi - G_2(\alpha R)] - \alpha^2 r^2 G_3(\alpha R)\} \hat{\mathbf{e}}_z + \alpha r [\xi - G_2(\alpha R)] \hat{\mathbf{e}}_\varphi, \quad (1.20)$$

where

$$G_3(u) = u^{-1} dG_2(u)/du = u^{-4}[(3 - u^2)u^{-1} \sin u - 3 \cos u]. \quad (1.21)$$

The vortex field corresponding to (1.20) has the form

$$\text{curl } \mathbf{V}_\xi(r, z) = \alpha^3 r z G_3(\alpha R) \hat{\mathbf{e}}_r + \{2\alpha[\xi - G_2(\alpha R)] - \alpha^3 r^2 G_3(\alpha R)\} \hat{\mathbf{e}}_z - r \alpha^2 G_2(\alpha R) \hat{\mathbf{e}}_\varphi. \quad (1.22)$$

Remark 2. The vector fields (1.20) and (1.22) satisfy Eq. (1.16). Both flows have invariant spheres $\mathbb{S}_{a_k}^2$ of radii $R = a_k$ obeying the equation $G_2(\alpha a_k) = \xi$ or $\psi(r, z) = 0$. The vortex field on the invariant spheres $\mathbb{S}_{a_k}^2$ is not poloidal for any $\xi \neq 0$ because the angular velocity of $\text{curl } \mathbf{V}_\xi(r, z)$ [Eq. (1.22)] on the spheres $\mathbb{S}_{a_k}^2$ is $-r \alpha^2 G_2(\alpha a_k) = -r \alpha^2 \xi \neq 0$. The fluid flow $\mathbf{V}_\xi(r, z)$ is purely poloidal on the invariant spheres $\mathbb{S}_{a_k}^2$ because its angular velocity is $\alpha r [\xi - G_2(\alpha a_k)] = 0$ since $G_2(\alpha a_k) = \xi$.

To study what vortex torus knots $K_{m,n}$ are realized for the fluid flow $\mathbf{V}_\xi(r, z)$ [Eq. (1.20)] inside the first invariant spheroid $\mathbb{B}_{a_1}^3$ of radius a_1 it is necessary to study the limit behavior of the pitch $p(\psi)$ [or the safety factor $q_h(\psi)$] in two cases: (a) when the nested tori $\mathbb{T}_\psi^2 \subset \mathbb{B}_{a_1}^3$ collapse onto the innermost vortex axis $\mathbb{S}_{\psi_m}^1$ having coordinates $(r = r_m, z = z_m, 0 \leq \varphi \leq 2\pi)$ and $\psi_m = \psi(r_m, z_m)$ and (b) when the invariant tori

$\mathbb{T}_\psi^2 \subset \mathbb{B}_{a_1}^3$ approach at $\psi \rightarrow 0$ their limit that is the union of the invariant sphere $\mathbb{S}_{a_1}^2$ and invariant diameter $r = 0$. In Moffatt's works [2–4] it is stated¹ that in case (a) the limit value of the pitch p is always equal to infinity and in case (b) the limit value of the pitch p is always equal to zero. In Secs. V and VI we prove that both statements are incorrect for the following physical reasons.

For case (a), in spite of the poloidal components of $\text{curl } \mathbf{V}_\xi(r, z)$ tending to zero near a vortex axis $\mathbb{S}_{\psi_m}^1$, the angular velocity of rotation of the poloidal projection (of the helical vortex line) around the point $a_m = (r_m, z_m)$ has a nonzero limit (in the nondegenerate case). This causes a finite and nonzero limit for the pitch p (and for the safety factor q_h) at the vortex axis.

For case (b) the invariant set defined by the equation $\psi(r, z) = 0$ inside the first invariant spheroid $\mathbb{B}_{a_1}^3$ is the union of the boundary sphere $\mathbb{S}_{a_1}^2$ and its diameter I that satisfies the equation $r = 0$ and connects two poles N and S on the sphere. Therefore, poloidal curves C_ψ at $\psi \rightarrow 0$ approach the union of the semicircle $\sqrt{r^2 + z^2} = a_1, r \geq 0$, and the diameter I : $r = 0$ and $-a_1 \leq z \leq a_1$. Since N and S belong to the sphere $\mathbb{S}_{a_1}^2$ where $\psi(r, z) = 0$ we get from (1.18) that at these points $G_2(\alpha a_1) = \xi$.² When $\psi \rightarrow 0$ the poloidal projections of the vortex filaments move along the meridians on the sphere $\mathbb{S}_{a_1}^2$ to a small neighborhood of the pole N . Then, after staying a long time T_N near the pole N the vortex filaments move along the diameter I to a small neighborhood of the pole S and the same dynamics repeats, etc. Formula (1.22) yields that the angular velocity of $\text{curl } \mathbf{V}_\xi(r, z)$ is $-\alpha^2 G_2(\alpha R)$, which near the poles N and S becomes approximately equal to $-\alpha^2 \xi$ because $G_2(\alpha a_1) = \xi$ at the points N and S . Therefore, during the long time T_N of a vortex line evolution near the poles N and S its pitch $p(\psi)$ [Eq. (1.8)] acquires a big change equal to

$$-2\alpha^2 G_2(\alpha R) T_N \approx -2\alpha^2 \xi T_N. \quad (1.23)$$

The contribution to the pitch $p(\psi)$ [Eq. (1.8)] from the evolution of vortex filament outside the poles N and S is much smaller than (1.23). Therefore, at $\psi \rightarrow 0$ the value of the pitch $p(\psi) \rightarrow +\infty$ if $\xi < 0$ and $p(\psi) \rightarrow -\infty$ if $\xi > 0$.

The formula (1.23) becomes an uncertainty when $\xi = 0$. For this case we prove in Sec. VI that the pitch $p(\psi)$ has a finite limit at $\psi \rightarrow 0$ and derive an exact formula for it.

Remark 3. For the magnetic field $\mathbf{B}_\xi(r, z)$ that has the same form as $\mathbf{V}_\xi(r, z)$ [Eq. (1.20)] the behavior of its pitch $p(\psi)$ at $\psi \rightarrow 0$ is completely different. The distinction is connected

¹In [2] on p. 129 about the pitch: “This quantity clearly increases continuously from zero to infinity as ψ increases from zero (on $R = a$) to ψ_{\max} (on the vortex axis)”. In [3] on p. 30 about the spheromak force-free magnetic field $\mathbf{B}(\mathbf{x})$: “Each \mathbf{B} -line is a helix and the pitch of the helices decreases continuously from infinity on the magnetic axis to zero on the sphere $r = R$ as we move outwards across the family of toroidal surfaces”.

²The poles N and S are the saddle stagnation points for the fluid flow $\mathbf{V}_\xi(\mathbf{x})$ (1.20) inside the spheroid $\mathbb{B}_{a_1}^3$. The diameter I is a fluid streamline that is a separatrix of the stagnation points N and S . The same points N and S are the focus-saddle stagnation points for the vortex field $\text{curl } \mathbf{V}_\xi(\mathbf{x})$.

with the fact that the vortex field $\text{curl } \mathbf{V}_\xi(r, z)$ [Eq. (1.22)] is not poloidal on the invariant sphere $\mathbb{S}_{a_1}^2$, while the fluid velocity field $\mathbf{V}_\xi(r, z)$ [and hence the magnetic field $\mathbf{B}_\xi(r, z)$] is purely poloidal (see Remark 2 above). Therefore, in MHD the limit of the safety factor $q(\psi)$ [Eq. (1.10)] at $\psi \rightarrow 0$ is finite for any ξ . Its exact formula is not included here.

Since the Stokes function (1.18) is a first integral of the fluid flow $\mathbf{V}_\xi(r, z)$ [Eq. (1.20)] and its vortex field (1.22), we get from (1.18) that roots a_k of the equation

$$G_2(\alpha a_k) = \xi \quad (1.24)$$

define spheroids $\mathbb{B}_{a_k}^3$ of radii $R = a_k$ that are invariant under the flows $\mathbf{V}_\xi(r, z)$ [Eq. (1.20)] and $\text{curl } \mathbf{V}_\xi(r, z)$ [Eq. (1.22)]. The flows possess invariant spheroids $\mathbb{B}_{a_k}^3$ only if the parameter ξ belongs to the range of function $G_2(u)$ since otherwise Eq. (1.24) does not have any roots. A calculation shows that the range of the function $G_2(u)$ is the segment $I^* = [-1/3, \xi_1 \approx 0.02872]$. Therefore, for $\xi < -1/3$ or $\xi > \xi_1$ the fluid flow $\mathbf{V}_\xi(r, z)$ [Eq. (1.20)] does not have any invariant spheroids.

For $\xi_1 < \xi < \bar{\xi}_1 \approx 0.11182$ the flows $\mathbf{V}_\xi(r, z)$ [Eq. (1.20)] and $\text{curl } \mathbf{V}_\xi(r, z)$ [Eq. (1.22)] have $K(\xi)$ disjoint invariant rings \mathcal{R}_i^3 . The number $K(\xi) = 3$ when $\xi \rightarrow \xi_1$, $\xi > \xi_1$ and $K(\xi) = 1$ for $\xi \rightarrow \bar{\xi}_1$, $\xi < \bar{\xi}_1$. We study fluid flows with $\xi_1 < \xi < \bar{\xi}_1$ in Sec. VII. For $\xi > \bar{\xi}_1$ or $\xi < -1/3$ the flows $\mathbf{V}_\xi(r, z)$ and $\text{curl } \mathbf{V}_\xi(r, z)$ do not have any invariant tori \mathbb{T}^2 and any closed vortex lines.

For $-1/3 < \xi < \xi_1$ and $\xi \neq 0$, the flows $\mathbf{V}_\xi(r, z)$ and $\text{curl } \mathbf{V}_\xi(r, z)$ in the whole Euclidean space \mathbb{R}^3 have a finite number $N(\xi)$ of nested invariant spheroids $\mathbb{B}_{a_k}^3$ and a finite number $K(\xi)$ of disjoint invariant rings \mathcal{R}_i^3 .

For $\xi = 0$, the exact solution (1.18) describes the spheromak fluid flow that was discovered first by Woltjer [16] as a plasma equilibrium and was applied by him to model a magnetic field in the Crab Nebula. The spheromak fluid flow $\mathbf{V}_0(r, z)$ has infinitely many nested invariant spheroids $\mathbb{B}_{a_k}^3$ with radii a_k satisfying the equation $\tan(\alpha a_k) = \alpha a_k$ and hence having the asymptotics $a_k \approx |\alpha|^{-1}(k + 1/2)\pi$ at $k \rightarrow \infty$. For $\xi \neq 0$ the number $N(\xi)$ of \mathbf{V}_ξ -invariant spheroids $\mathbb{B}_{a_k}^3$ is finite and $N(\xi) \rightarrow \infty$ when $\xi \rightarrow 0$. For positive ξ , $0 < \xi < \xi_1$, the number $N(\xi)$ is even; for negative ξ , $-1/3 < \xi < 0$, the number $N(\xi)$ is odd. These facts follow at once from the plot of function $y_1(u) = G_2(u)$ in Fig. 1 and Eq. (1.24).

The Prendergast exact solution [17] describes plasma equilibrium with everywhere vanishing fluid velocity $\mathbf{V}(\mathbf{x}) \equiv 0$ or a hydrostatic model of a magnetic star.

Section VIII is devoted to a liquid planet model. Here the necessary boundary conditions of vanishing of fluid velocity $\mathbf{V}_\xi(\mathbf{x})$ and pressure $p(\mathbf{x})$ on the surface $\mathbb{S}_{a_\ell}^2$ ($|\mathbf{x}| = a_\ell$) of the planet are satisfied for special values of the parameter $\xi = \xi_\ell$. The numbers $\xi_\ell = G_2(u_\ell)$ are extremal values of the function $G_2(u)$ (local maxima and local minima) that are attained at the points u_ℓ satisfying the equation $G_3(u_\ell) = u_\ell^{-1}G_2'(u_\ell) = 0$.

In Secs. V–VII we give a complete classification of all vortex knots for the fluid flows $\mathbf{V}_\xi(r, z)$ [Eq. (1.20)]. Additionally, these results provide counterexamples to the Moffatt statements of [2–4] on vortex knots.

The moduli spaces of vortex knots are defined and studied in [18] for the exact Beltrami flow having stream function $\psi(r, z) = -zr^2G_3(R)$. Reference [19] is devoted to the investi-

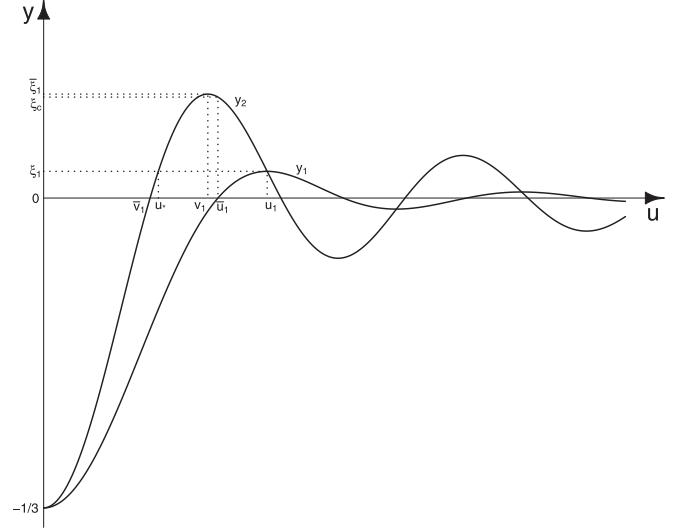


FIG. 1. Plot of the functions $y_1(u) = G_2(u)$ and $y_2(u) = -[G_1(u) + G_2(u)]/2$.

gation of the moduli spaces of vortex knots for the spheromak fluid flow that has the stream function $\psi(r, z) = -r^2G_2(R)$. The results of [18, 19] are equally applicable to the analogous force-free plasma equilibria.

II. LIMIT OF THE PITCH FUNCTION AT A VORTEX AXIS

The dynamical system of vortex lines $d\mathbf{x}/dt = \text{curl } \mathbf{V}$ has the form

$$\frac{d\mathbf{x}}{dt} = \frac{d}{dt}(x\hat{\mathbf{e}}_x + y\hat{\mathbf{e}}_y + z\hat{\mathbf{e}}_z) = r\hat{\mathbf{e}}_r + r\dot{\varphi}\hat{\mathbf{e}}_\varphi + \dot{z}\hat{\mathbf{e}}_z = \text{curl } \mathbf{V}. \quad (2.1)$$

This equation by virtue of Eqs. (1.3) and (1.7) yields

$$\dot{r} = -\frac{1}{r}C'(\psi)\psi_z, \quad \dot{z} = \frac{1}{r}C'(\psi)\psi_r, \quad (2.2)$$

$$\dot{\varphi} = -H'(\psi) + \frac{1}{r^2}C(\psi)C'(\psi). \quad (2.3)$$

Suppose that the stream function $\psi(r, z)$ has a local non-degenerate maximum or minimum $\psi_m = \psi(a_m)$ at a point $a_m = (r_m, z_m)$:

$$\begin{aligned} \psi_r(a_m) &= 0, & \psi_z(a_m) &= 0, \\ \mathcal{H}(a_m) &= \psi_{rr}(a_m)\psi_{zz}(a_m) - \psi_{rz}^2(a_m) > 0. \end{aligned} \quad (2.4)$$

Hence the system (2.2) has the center equilibrium point a_m and the system (2.2) and (2.3) has a stable trajectory-vortex axis $\mathbb{S}_{\psi_m}: r = r_m, z = z_m, 0 \leq \varphi < 2\pi$, and $\psi_m = \psi(r_m, z_m)$. All trajectories of the system (2.2) near the center are closed curves C_ψ , $\psi(r, z) = \text{const}$, encircling the point a_m . The corresponding trajectories of the system (2.2) and (2.3) are either infinite helices or closed curves (knots) lying on the invariant tori $\mathbb{T}_\psi^2 = C_\psi \times \mathbb{S}^1$, where the circle \mathbb{S}^1 corresponds to the angular variable φ .

Substituting Eq. (2.3) into the formula (1.8), we get

$$p(\psi) = -H'(\psi)t(\psi) + C(\psi)C'(\psi) \int_0^{t(\psi)} \frac{dt}{r^2(t)}. \quad (2.5)$$

331 In the limit $\psi \rightarrow \psi_m$ we have $r(t) \rightarrow r_m$ for all t , hence

$$p(\psi_m) = \lim_{\psi \rightarrow \psi_m} p(\psi) = t(\psi_m) \left[-H'(\psi_m) + C(\psi_m)C'(\psi_m)/r_m^2 \right], \quad (2.6)$$

332 where $t(\psi_m) = \lim_{\psi \rightarrow \psi_m} t(\psi)$.

333 The dynamical system (2.2) near the equilibrium point
334 (r_m, z_m) is approximated by the system in variations [20]

$$\frac{d\delta r}{dt} = -a_{11}\delta z - a_{12}\delta r, \quad \frac{d\delta z}{dt} = a_{12}\delta z + a_{22}\delta r, \quad (2.7)$$

$$a_{11} = c_m \psi_{zz}(a_m), \quad a_{12} = c_m \psi_{rz}(a_m), \quad a_{22} = c_m \psi_{rr}(a_m),$$

$$c_m = \frac{C'(\psi_m)}{r_m}, \quad (2.8)$$

335 where $\delta r(t) = r(t) - r_m$ and $\delta z(t) = z(t) - z_m$. From
336 Eqs. (2.4) and (2.8) we get

$$D_m = a_{11}a_{22} - a_{12}^2 = c_m^2 \mathcal{H}(a_m) > 0. \quad (2.9)$$

337 The linear system (2.7) has the quadratic first integral
338 $Q(\delta r, \delta z) = a_{22}(\delta r)^2 + 2a_{12}\delta r\delta z + a_{11}(\delta z)^2$ that in view of
339 (2.9) is either positive or negative definite. Hence its level
340 curves $Q(\delta r, \delta z) = \text{const}$ are nested ellipses and therefore all
341 solutions to (2.7) are periodic. Due to the scaling invariance of
342 the linear system (2.7), all its solutions have the same period
343 $t_m = 2\pi/\sqrt{D_m}$.

344 From the general theory of dynamical systems [20] it
345 follows that the limit at $\psi \rightarrow \psi_m$ of the function of periods
346 $t(\psi)$ is the period t_m of the system in variations (2.7). Using
347 formula (2.9) we find

$$t(\psi_m) = \lim_{\psi \rightarrow \psi_m} t(\psi) = \frac{2\pi}{\sqrt{D_m}} = \frac{2\pi r_m}{|C'(\psi_m)|\sqrt{\mathcal{H}(a_m)}}. \quad (2.10)$$

348 Substituting (2.10) into (2.6) we get

$$p(\psi_m) = \lim_{\psi \rightarrow \psi_m} p(\psi) = \frac{2\pi r_m}{|C'(\psi_m)|\sqrt{\mathcal{H}(a_m)}} \left[-H'(\psi_m) + \frac{1}{r_m^2} C(\psi_m)C'(\psi_m) \right]. \quad (2.11)$$

349 Formula (2.11) shows that the Moffatt statement of [2–4] that
350 at the vortex axis the pitch p is always equal to infinity can be
351 true only for degenerate solutions with either $C'(\psi_m) = 0$ or
352 $\mathcal{H}(a_m) = 0$.

353 Using Eq. (1.3) we find

$$-H'(\psi_m) + \frac{1}{r_m^2} C(\psi_m)C'(\psi_m) = -\frac{1}{r_m^2} \left(\psi_{rr} - \frac{1}{r} \psi_r + \psi_{zz} \right) (a_m). \quad (2.12)$$

354 At the equilibrium point a_m in view of $\psi_r(a_m) = 0$ we have

$$\left(\psi_{rr} - \frac{1}{r} \psi_r + \psi_{zz} \right) (a_m) = \left(\psi_{rr} + \frac{1}{r} \psi_r + \psi_{zz} \right) (a_m) = \Delta \psi(a_m), \quad (2.13)$$

355 where Δ is the Laplace operator. Substituting (2.12) and
356 (2.13) into Eq. (2.11) we get, for the safety factor

$$q_h(\psi_m) = p(\psi_m)/2\pi, \quad 357$$

$$q_h(\psi_m) = -\frac{\Delta \psi(a_m)}{r_m C'(\psi_m) \sqrt{\mathcal{H}(a_m)}}. \quad (2.14)$$

The derivatives $\psi_{rr}(a_m)$ and $\psi_{zz}(a_m)$ have the same sign since
the point a_m is either a local maximum or a local minimum
of the function $\psi(r, z)$. Hence, using the standard inequality
we find

$$\begin{aligned} \sqrt{\mathcal{H}(a_m)} &= \sqrt{\psi_{rr}(a_m)\psi_{zz}(a_m) - \psi_{rz}^2(a_m)} \\ &\leq \sqrt{\psi_{rr}(a_m)\psi_{zz}(a_m)} \leq |\psi_{rr}(a_m) + \psi_{zz}(a_m)|/2 \\ &= |\Delta \psi(a_m)|/2. \end{aligned}$$

Applying this inequality in (2.14) we derive

$$|q_h(\psi_m)| \geq \frac{2}{r_m |C'(\psi_m)|}. \quad (2.15)$$

For $C(\psi) = \alpha\psi$ we get the simple formula $|q_h(\psi_m)| \geq$
 $2(|\alpha|r_m)^{-1}$.

Formulas (2.14) and (2.15) prove that for the case of
arbitrary functions $H(\psi)$ and $C(\psi)$ in Eq. (1.3) the safety
factor $q_h(\psi)$ has a finite and nonzero limit at $\psi \rightarrow \psi_m$
provided the nondegeneracy conditions $C'(\psi_m) \neq 0$, $\mathcal{H}(a_m) \neq 0$
are met. The limit (2.14) is one of the two bounds of the range
of safety factor $q_h(\psi)$. Hence we get one of the two bounds
of safety factor $q_h(\psi)$ for the range of the rational values m/n corresponding
to the torus knots $K_{m,n}$ that can be realized as vortex knots for
the considered fluid flow $\mathbf{V}(\mathbf{x})$ [Eq. (1.2)].

III. LIMIT OF THE SAFETY FACTOR AT A MAGNETIC AXIS

Equations of magnetohydrodynamics have the form

$$\begin{aligned} \frac{\partial \mathbf{V}}{\partial t} + \text{curl} \mathbf{V} \times \mathbf{V} &= -\text{grad} \left(\frac{p}{\rho} + \frac{1}{2} |\mathbf{V}|^2 + \Phi \right) \\ &\quad + \frac{1}{\rho \mu} \text{curl} \mathbf{B} \times \mathbf{B} + \nu \Delta \mathbf{V}, \\ \frac{\partial \mathbf{B}}{\partial t} &= \text{curl}(\mathbf{V} \times \mathbf{B}), \quad \text{div} \mathbf{V} = 0, \quad \text{div} \mathbf{B} = 0, \end{aligned} \quad (3.1)$$

where \mathbf{B} is the magnetic field, μ the magnetic permeability, ν
the kinematic viscosity, and Δ the Laplace operator. As known
since the Newcomb paper [21], Eqs. (3.1) imply that magnetic
field $\mathbf{B}(t, \mathbf{x})$ is transformed in time by the flow diffeomorphisms
or is frozen in the flow. Therefore, in the MHD any magnetic
field \mathbf{B} knot is transformed in time into an isotopic \mathbf{B} knot.

Plasma equilibrium equations follow from (3.1) for $\mathbf{V} = 0$:

$$\text{curl} \mathbf{B} \times \mathbf{B} = \text{grad}(\mu p + \rho \mu \Phi), \quad \text{div} \mathbf{B} = 0. \quad (3.2)$$

The hydrodynamics equilibrium equations follow from (3.1)
for $\mathbf{B} = 0$:

$$\text{curl} \mathbf{V} \times \mathbf{V} = \text{grad} \left(-\frac{p}{\rho} - \Phi - \frac{1}{2} |\mathbf{V}|^2 \right), \quad \text{div} \mathbf{V} = 0. \quad (3.3)$$

Since Eqs. (3.2) and (3.3) are equivalent [5], we get that for
the axisymmetric solutions the same ψ functions satisfying
Eq. (1.3) describe axisymmetric equilibria of ideal fluid and

389 plasma. Topological invariants of the equilibrium of fluid are
390 defined by the curl \mathbf{V} knots, while the topological invariants of
391 plasma equilibrium are defined by the \mathbf{B} knots.

392 Let us show that these topological invariants for the ideal
393 fluid and for plasma are completely different, for the same ψ
394 function $\psi(r, z)$. Indeed, the axisymmetric magnetic field $\mathbf{B}(\mathbf{x})$
395 has a form analogous to (1.2),

$$\mathbf{B}(r, z) = -\frac{1}{r} \frac{\partial \psi}{\partial z} \hat{\mathbf{e}}_r + \frac{1}{r} \frac{\partial \psi}{\partial r} \hat{\mathbf{e}}_z + \frac{C(\psi)}{r} \hat{\mathbf{e}}_\varphi, \quad (3.4)$$

396 where we used the second of Eqs. (1.4), which follows from
397 (3.2). The corresponding dynamical system of magnetic field
398 lines $d\mathbf{x}/dt = \mathbf{B}(\mathbf{x})$ is

$$\dot{r} = -\psi_z/r, \quad \dot{z} = \psi_r/r, \quad (3.5)$$

$$\dot{\varphi} = C(\psi)/r^2. \quad (3.6)$$

399 For closed magnetic field lines on an invariant torus \mathbb{T}_ψ^2
400 that go around the torus m times the long way around and
401 n times the short way around, the *safety factor* q is defined
402 as $q = m/n$ [9,12,22]. Mercier had demonstrated in [9] that
403 the value of the safety factor q is connected with stability of
404 the MHD equilibria: For example, if $q = 1/n$, where n is an
405 integer, then the MHD equilibrium is unstable.

406 For the axisymmetric magnetic fields the definition of
407 [9,12,22] conforms to the definition (1.10), which after
408 substituting Eq. (3.6) gives

$$q(\psi) = \frac{1}{2\pi} C(\psi) \int_0^{t(\psi)} \frac{dt}{r^2(t)}. \quad (3.7)$$

409 The analogous safety factor in hydrodynamics $q_h(\psi) =$
410 $p(\psi)/(2\pi)$ due to Eq. (2.5) is

$$q_h(\psi) = \frac{1}{2\pi} \left[-H'(\psi)t(\psi) + C(\psi)C'(\psi) \int_0^{t(\psi)} \frac{dt}{r^2(t)} \right]. \quad (3.8)$$

411 For the same closed trajectory C_ψ , $\psi(r, z) = \text{const}$, the two
412 safety factors $q(\psi)$ and $q_h(\psi)$ are qualitatively different. For
413 example, when $q(\psi)$ [Eq. (3.7)] is a rational number m/n
414 and hence the corresponding magnetic field \mathbf{B} line is a torus
415 knot $K_{m,n}$ [9,12], the safety factor $q_h(\psi)$ [Eq. (3.8)] in general
416 is an irrational number and the corresponding curl \mathbf{V} line is
417 an infinite curve dense on the invariant torus $\mathbb{T}_\psi^2 = C_\psi \times \mathbb{S}^1$
418 and vice versa. Here the circle \mathbb{S}^1 corresponds to the angular
419 variable φ . Another possibility appears when both safety
420 factors are rational numbers, $q(\psi) = m/n$ and $q_h(\psi) = p/q$,
421 and therefore define topologically nonequivalent torus knots:
422 the magnetic field \mathbf{B} knot $K_{m,n}$ and the vortex knot $K_{p,q}$.

423 Let the magnetic field $\mathbf{B}(\mathbf{x})$ have a family of nested invariant
424 tori \mathbb{T}_ψ^2 defined by the equation $\psi = \text{const}$. Then the innermost
425 torus $\mathbb{T}_{\psi_m}^2$ is a circle $\mathbb{S}_{\psi_m}^1$, which is called a magnetic axis
426 $\psi = \psi_m$. The magnetic axis corresponds to a center equilib-
427 rium point $a_m = (r_m, z_m)$ of the system (3.5), which is defined
428 by the same equations (2.4) as for the stable vortex axis in
429 hydrodynamics. The safety factor (3.7) at $\psi \rightarrow \psi_m$ due to
430 $r(t) \rightarrow r_m$ has the limit

$$q(\psi_m) = \lim_{\psi \rightarrow \psi_m} q(\psi) = \frac{1}{2\pi r_m^2} \overline{t(\psi_m)} C(\psi_m), \quad (3.9)$$

where $\overline{t(\psi_m)} = \lim_{\psi \rightarrow \psi_m} \overline{t(\psi)}$. To derive the limit value $\overline{t(\psi_m)}$ 431
we consider the system in variations for the system (3.5) near 432
its stable equilibrium a_m : 433

$$\frac{d\delta r}{dt} = -b_{11}\delta z - b_{12}\delta r, \quad \frac{d\delta z}{dt} = b_{12}\delta z + b_{22}\delta r, \quad (3.10)$$

$$b_{11} = \psi_{zz}(a_m)/r_m, \quad b_{12} = \psi_{rz}(a_m)/r_m, \quad b_{22} = \psi_{rr}(a_m)/r_m. \quad (3.11)$$

Here $\delta r(t) = r(t) - r_m$ and $\delta z(t) = z(t) - z_m$. From (2.4) and 434
(3.11) we find 435

$$\overline{D_m} = b_{11}b_{22} - b_{12}^2 = \mathcal{H}(a_m)/r_m^2 > 0. \quad (3.12)$$

Due to the inequality (3.12) and the scaling invariance of the 436
linear system (3.10), all its trajectories have the same period 437
 $\overline{t_m} = 2\pi/\sqrt{\overline{D_m}} = 2\pi r_m/\sqrt{\mathcal{H}(a_m)}$. 438

From the general theory of dynamical systems [20] we get 439
that the limit at $\psi \rightarrow \psi_m$ of the function of periods $\overline{t(\psi)}$ is the 440
period $\overline{t_m}$ of the system in variations (3.10). Hence $\overline{t(\psi_m)} =$ 441
 $\lim_{\psi \rightarrow \psi_m} \overline{t(\psi)} = \overline{t_m} = 2\pi r_m/\sqrt{\mathcal{H}(a_m)}$. Substituting into (3.9) 442
we get the limit value of the safety factor 443

$$q(\psi_m) = \frac{C(\psi_m)}{r_m \sqrt{\mathcal{H}(a_m)}} \quad (3.13)$$

at the magnetic axis $\psi = \psi_m$. 444

At the vortex axis $\psi = \psi_m$, the hydrodynamic safety factor 445
 $q_h(\psi) = p(\psi)/2\pi$ in view of (2.11) and (3.13) has the limit 446

$$q_h(\psi_m) = q(\psi_m) - \frac{r_m H'(\psi_m)}{C'(\psi_m) \sqrt{\mathcal{H}(a_m)}}. \quad (3.14)$$

The limit safety factors (3.13) and (3.14) are evidently 447
different. 448

For the solutions satisfying Eqs. (1.14) and (1.15) we find 449

$$q(\psi_m) = \frac{\alpha \psi_m}{r_m \sqrt{\mathcal{H}(a_m)}}, \quad q_h(\psi_m) = \frac{\alpha(\psi_m - \xi r_m^2)}{r_m \sqrt{\mathcal{H}(a_m)}}. \quad (3.15)$$

Formulas (3.15) show that the two safety factors $q(\psi_m)$ and 450
 $q_h(\psi_m)$ are different if $\xi \neq 0$ and coincide if $\xi = 0$. 451

IV. MAIN DYNAMICAL SYSTEM 452

Moffatt studied in [2] vortex lines for the exact solutions to 453
Eq. (1.15): 454

$$\psi(r, z) = r^2 \left[\frac{\lambda}{\alpha^2} + A \left(\frac{a}{R} \right)^{3/2} J_{3/2}(\alpha R) \right], \quad R = \sqrt{r^2 + z^2}, \quad (4.1)$$

where $J_\nu(u)$ is the Bessel function of order ν . The solutions 455
[Eq. (54) of [2]] are considered in [2] for 456

$$\frac{\lambda}{\alpha^2} = -A J_{3/2}(\alpha a) \quad (4.2)$$

[Eq. (57) of [2]] in the first invariant spheroid \mathbb{B}_a ($R \leq a$), 457
where the vortex lines on the invariant tori $\mathbb{T}_\psi^2 \subset \mathbb{B}_a$ are either 458
infinite helices or torus knots $K_{m,n}$. The solutions (4.1) and 459
(4.2) are matched continuously with an irrotational flow for 460
 $R > a$ having the stream function 461

$$\psi(r, z) = -\frac{1}{3} A J_{5/2}(\alpha a) r^2 \left(1 - \frac{a^3}{R^3} \right).$$

The solutions (4.1) and (4.2) with $J_{5/2}(\alpha a) = 0$ were derived by Prendergast [17] as a model of equilibrium of a magnetic star; the continuously matched exterior magnetic field \mathbf{B} vanishes in view of the condition $J_{5/2}(\alpha a) = 0$. For $\lambda = 0$, the flux function (4.1) describes the spheromak magnetic field \mathbf{B} [by the same formula as (1.2)] that was discovered first by Woltjer [16] and applied by him to model the Crab Nebula (see also [23]).

In Ref. [2] (pp. 128–129) Moffatt writes about the pitch $p(\psi)$ of the helical vortex lines: “This quantity clearly increases continuously from zero to infinity as ψ increases from zero (on $R = a$) to ψ_{\max} (on the vortex axis)”. Thus Moffatt states here that for all values of the parameters A , α , and $\lambda/\alpha^2 = -AJ_{3/2}(\alpha a)$ [formula (57) of [2]] the limits of the pitch function $p(\psi)$ at $\psi \rightarrow 0$ and at $\psi \rightarrow \psi_{\max}$ are

$$p(0) = \lim_{\psi \rightarrow 0} p(\psi) = 0, \quad p(\psi_{\max}) = \lim_{\psi \rightarrow \psi_{\max}} p(\psi) = \infty.$$

The same results for the Beltrami vector fields [having stream functions (4.1) with $\lambda = 0$] are stated in [3] (pp. 30–31).

Our formula (2.11) $\lim_{\psi \rightarrow \psi_m} p(\psi) = p(\psi_m) < \infty$ is rigorously proven in Sec. II for any axisymmetric flows (1.2). Formula (2.11) demonstrates that presented in [2,3] Moffatt’s statement that $\lim_{\psi \rightarrow \psi_{\max}} p(\psi) = \infty$ does not correspond to the facts.

The known formula for the Bessel functions $J_{n+1/2}(u)$ yields (see [24], p. 56)

$$J_{3/2}(u) = -\frac{1}{\sqrt{\pi/2}\sqrt{u}} \left(\cos u - \frac{\sin u}{u} \right).$$

Therefore, the solution (54) of [2] [formula (4.1) above] takes the form

$$\psi(r, z) = r^2 \left[\frac{\lambda}{\alpha^2} - \frac{A(|\alpha|a)^{3/2}}{\sqrt{\pi/2}(\alpha R)^2} \left(\cos(\alpha R) - \frac{\sin(\alpha R)}{(\alpha R)} \right) \right]. \quad (4.3)$$

Instead of Bessel’s functions $J_{n+1/2}(u)$ we will use the elementary functions

$$\begin{aligned} G_0(u) &= -\cos u, \quad G_1(u) = \frac{d}{udu} G_0(u) = \frac{\sin u}{u} \\ &= \frac{\sqrt{\pi/2}}{u^{1/2}} J_{1/2}(u), \\ G_2(u) &= \frac{d}{udu} G_1(u) = \frac{1}{u^2} \left[\cos u - \frac{\sin u}{u} \right] = -\frac{\sqrt{\pi/2}}{u^{3/2}} J_{3/2}(u), \\ G_3(u) &= \frac{d}{udu} G_2(u) = \frac{1}{u^4} \left[(3 - u^2) \frac{\sin u}{u} - 3 \cos u \right] \\ &= \frac{\sqrt{\pi/2}}{u^{5/2}} J_{5/2}(u), \\ G_4(u) &= \frac{1}{u} \frac{dG_3(u)}{du} \\ &= \frac{1}{u^6} \left[(6u^2 - 15) \frac{\sin u}{u} - (u^2 - 15) \cos u \right]. \quad (4.4) \end{aligned}$$

All functions $G_n(u)$ are analytic everywhere and have the values

$$\begin{aligned} G_1(0) &= 1, \quad G_2(0) = -1/3, \quad G_3(0) = 1/15, \\ G_4(0) &= -1/105. \end{aligned} \quad (4.5)$$

The functions $G_n(u)$ [Eq. (4.4)] satisfy the easily verifiable identities

$$G_0 + G_1 + u^2 G_2 = 0, \quad G_1 + 3G_2 + u^2 G_3 = 0. \quad (4.6)$$

The general identity is $G_n + (2n + 1)G_{n+1} + u^2 G_{n+2} = 0$, with $G_{n+1} = u^{-1} dG_n/du$.

The stream function (4.3) in view of (4.4) takes the form

$$\begin{aligned} \psi(r, z) &= Br^2[\xi - G_2(\alpha R)], \quad B = \frac{A(|\alpha|a)^{3/2}}{\sqrt{\pi/2}}, \\ \xi &= \frac{\lambda}{\alpha^2 B} = \frac{\lambda\sqrt{\pi/2}}{A|\alpha|^{7/2}a^{3/2}}. \end{aligned} \quad (4.7)$$

Hence we get, for $H(\psi) = \lambda\psi$ and $C(\psi) = \alpha\psi$,

$$-H'(\psi) + \frac{1}{r^2} C(\psi)C'(\psi) = -\lambda + \frac{\alpha^2}{r^2} \psi = -\alpha^2 B G_2(\alpha R). \quad (4.8)$$

Substituting $C(\psi) = \alpha\psi$ and (4.8) into the system (2.2) and (2.3) we get, for the main dynamical system (2.1),

$$\dot{r} = -\frac{\alpha}{r} \psi_z, \quad \dot{z} = \frac{\alpha}{r} \psi_r, \quad \dot{\psi} = -\alpha^2 B G_2(\alpha R).$$

Substituting here formulas (4.7) and (4.4) we get

$$\begin{aligned} \dot{r} &= \alpha^3 Brz G_3(\alpha R), \\ \dot{z} &= 2\alpha B[\xi - G_2(\alpha R)] - \alpha^3 Br^2 G_3(\alpha R), \\ \dot{\psi} &= -\alpha^2 B G_2(\alpha R). \end{aligned} \quad (4.9)$$

The parameters α and B are nonessential here because they can be removed by the scaling transformation $r_1 = |\alpha|r$, $z_1 = |\alpha|z$, and the time change $d\tau/dt = \alpha^2 B$. Therefore, we assume $B > 0$, which means $A > 0$ [Eq. (4.7)]. The only essential parameter of the problem is the parameter $\xi = \lambda/\alpha^2 B$ [Eq. (4.7)].

Let us consider the system (4.9) and (4.10) in the first spheroid \mathbb{B}_a ($R \leq a$) that is invariant under the system. That means $\psi(r, z) = 0$ on the sphere \mathbb{S}_a^2 of radius $R = a$. Hence we get the condition $|\alpha|a = \bar{u}_1(\xi)$ where $\bar{u}_1(\xi)$ is the first root of the equation

$$G_2(u) = \xi. \quad (4.11)$$

Figure 1 shows that the range of the function $G_2(u)$ for all positive u is the segment I^* , $[-1/3, \xi_1]$, where ξ_1 is the maximal value of the function $G_2(u)$. The maximum is attained at a point u_1 where the derivative $G_2'(u)$ vanishes, $\xi_1 = G_2(u_1)$. Hence, from (4.4) we get $G_3(u_1) = u_1^{-1} G_2'(u_1) = 0$. The first root of the equation $G_3(u) = 0$ is $u_1 \approx 5.7635$. Hence we find the value of $\xi_1 = G_2(u_1) \approx 0.02872$. As a consequence we get that Eq. (4.11) has no solutions if $\xi < -1/3$ or $\xi > \xi_1$. Hence the fluid flow (1.2) and (4.1) does not have any invariant spheroid \mathbb{B}_c ($R \leq c$) if $\xi < -1/3$ or $\xi > \xi_1$.

From Fig. 1 we see that $\bar{u}_1(\xi) \in [0, u_1 \approx 5.7635]$. Figure 1 yields that Eq. (4.11) for $\xi \neq 0$ has a finite number $N(\xi)$ of roots and that $N(\xi) \rightarrow \infty$ when $\xi \rightarrow 0$. This means that the system (4.9) and (4.10) in the whole space \mathbb{R}^3 can have, for $\xi \neq 0$, a finite number $N(\xi)$ of invariant spheroids \mathbb{B}_{R_i} and has infinitely many invariant spheroids when $\xi = 0$. We consider the systems (4.9) and (4.10) in the spheroid \mathbb{B}_{R_1} ,

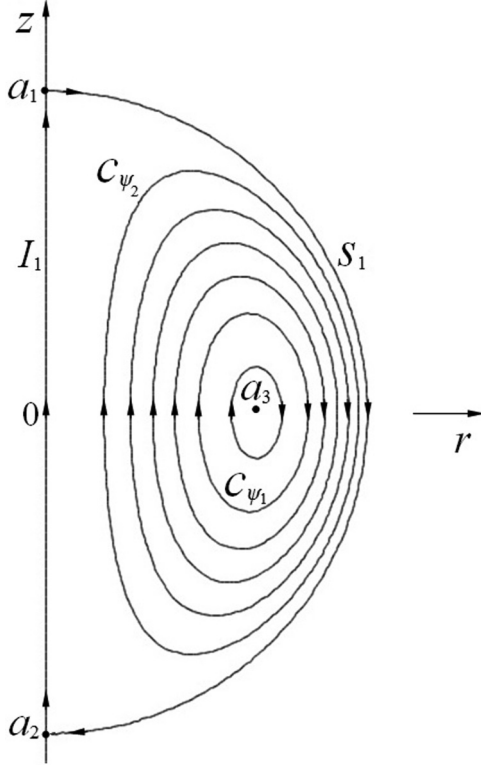


FIG. 2. Poloidal contours of stream surfaces inside the first invariant spheroid $\mathbb{B}_{a_1}^3$ for $-1/3 < \xi \leq \xi_1$. Rotation of contours around the z axis defines \mathbf{V} -invariant tori \mathbb{T}^2 . Rotation of the separatrix S_1 gives the \mathbf{V} -invariant sphere $\mathbb{S}_{a_1}^2$. Rotation of point a_3 produces the stable vortex axis $a_3 \times \mathbb{S}^1$.

529 $R_1 = a$, corresponding to the first root $\bar{u}_1(\xi)$ of Eq. (4.11);
 530 then $|\alpha| = \bar{u}_1(\xi)/a$. The first zero of the function $G_2(u)$ is
 531 $\bar{u}_1(0) = \bar{u}_1 \approx 4.4931$.

532 For $\xi \in I^*$ the system (4.9) and (4.10) has an invariant
 533 spheroid \mathbb{B}_a , $|\alpha|a = \bar{u}_1(\xi)$. The system (4.9) in the invariant
 534 semidisk D_1 [$\psi(r, z) \geq 0, r \geq 0, R \leq a$] has three equilibrium
 535 points: $a_1(r = 0, z = a)$, $a_2(r = 0, z = -a)$, $a_3(r = u_m/|\alpha|,$
 536 $z = 0)$. The equilibria a_1 and a_2 are nondegenerate saddles
 537 if $G_3[\bar{u}_1(\xi)] \neq 0$. Their separatrices are the interval I_1 , ($r =$
 538 $0, -a < z < a$), and the arc S_1 , ($r^2 + z^2 = a^2, r > 0$) (see
 539 Fig. 2). The equilibrium a_3 is a center, its coordinate $r =$
 540 $R_m = u_m(\xi)/|\alpha|$, where $u_m(\xi)$ is the first positive root of the
 541 equation $2G_2(u) + u^2G_3(u) = 2\xi$ (the condition that $\dot{z} = 0$ in
 542 (4.9) at the point $[a_3(r = R_m, z = 0), u = \alpha R]$). The latter in
 543 view of the second identity (4.6) takes the form

$$-[G_1(u) + G_2(u)]/2 = \xi. \quad (4.12)$$

544 All equilibrium points of the system (4.9) with $r \neq 0$ satisfy
 545 the equation $z = 0$ and Eq. (4.12) for $u = |\alpha|r$.

546 From Fig. 1 it follows that the range of the func-
 547 tion $-[G_1(u) + G_2(u)]/2$ for all positive u is the seg-
 548 ment $[-1/3, \xi_1]$ where ξ_1 is its maximum that is attained at
 549 a point v_1 ; hence we have $G'_1(v_1) + G'_2(v_1) = 0$. Equa-
 550 tions (4.4) yield $G'_1(u) + G'_2(u) = u[G_2(u) + G_3(u)]$; there-
 551 fore $G_2(v_1) + G_3(v_1) = 0$. The first root of this equation is
 552 $v_1 \approx 4.2329$. Hence we get $\bar{\xi}_1 = -2^{-1}[G_1(v_1) + G_2(v_1)] \approx$
 553 0.11182 .

V. KEY FUNCTION $f(\xi)$

554

Let us derive exact formulas for $p(\psi_m)$ [Eq. (2.11)] for
 555 solutions (4.7). Substituting $r^2 = R^2 - z^2$ into (4.7) and using
 556 the first identity (4.6) we find
 557

$$\psi(r, z) = B \left[\xi r^2 + \frac{1}{\alpha^2} [G_0(\alpha R) + G_1(\alpha R)] + z^2 G_2(\alpha R) \right]. \quad (5.1)$$

Differentiating the function $\psi(r, z)$ [Eq. (5.1)] and using
 558 formulas (4.4) we get
 559

$$\begin{aligned} \frac{\partial \psi}{\partial r} &= rB[2\xi + G_1(\alpha R) + G_2(\alpha R) + \alpha^2 z^2 G_3(\alpha R)], \\ \frac{\partial \psi}{\partial z} &= zB[G_1(\alpha R) + 3G_2(\alpha R) + \alpha^2 z^2 G_3(\alpha R)]. \end{aligned} \quad (5.2)$$

The function $\psi(r, z)$ [Eq. (4.7)] achieves its maximal in
 560 the semidisk D_1 value ψ_m at the point $a_3 = (r_m, z_m)$. Since
 561 $\psi_r(a_3) = 0$ and $\psi_z(a_3) = 0$, we get from (5.2) $z_m = 0$ and
 562 $u_m(\xi) = |\alpha|r_m$ satisfies Eq. (4.12). For the second derivatives
 563 of the function $\psi(r, z)$ at the point a_3 we find from (5.2)
 564

$$\begin{aligned} \psi_{rr}(a_3) &= u_m^2 B [G_2(u_m) + G_3(u_m)], \\ \psi_{zz}(a_3) &= B [G_1(u_m) + 3G_2(u_m)], \end{aligned} \quad (5.3)$$

with $\psi_{rz}(a_3) = 0$. Hence we get the Hessian (2.4),
 565

$$\mathcal{H}(a_m) = u_m^2 B^2 [G_2(u_m) + G_3(u_m)][G_1(u_m) + 3G_2(u_m)]. \quad (5.4)$$

Using formula (4.8) we find, on the vortex axis S_m [$\alpha R =$
 566 $u_m(\xi), z = 0$],
 567

$$-H'(\psi_m) + \frac{1}{r_m^2} C(\psi_m) C'(\psi_m) = -\alpha^2 B G_2(u_m(\xi)). \quad (5.5)$$

Substituting (5.4) and (5.5) and $r_m = u_m(\xi)/|\alpha|$ into (2.11),
 568 we find for the exact solutions (4.7)
 569

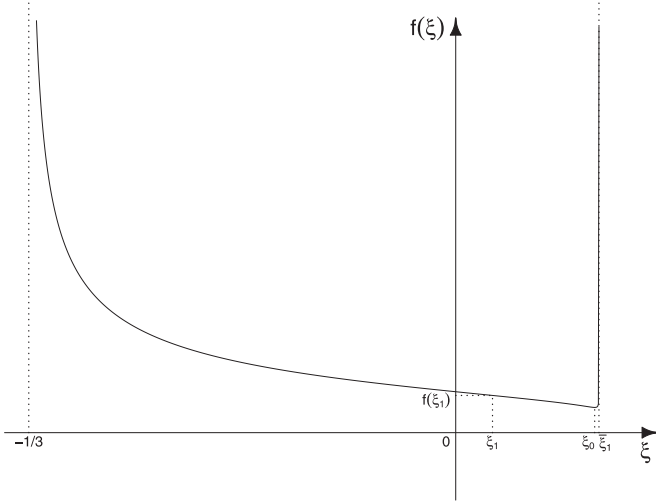
$$\begin{aligned} p(\psi_m) &= \lim_{\psi \rightarrow \psi_m} p(\psi) \\ &= -\frac{2\pi G_2(u_m)}{\sqrt{[G_2(u_m) + G_3(u_m)][G_1(u_m) + 3G_2(u_m)]}}. \end{aligned} \quad (5.6)$$

It is evident that formula (5.6) does not contain the two
 570 nonessential parameters α and B . Therefore, expression (5.6)
 571 is a function of the parameter ξ only, since $u_m = u_m(\xi)$ is a
 572 function of ξ defined as the first root of Eq. (4.12). Thus we
 573 arrive at the key function $f(\xi) = p(\psi_m(\xi))/2\pi = q_h(\psi_m(\xi))$.
 574 Applying the second identity (4.6), we get from (5.6)
 575

$$f(\xi) = -\frac{G_2(u_m(\xi))}{u_m(\xi) \sqrt{-G_3(u_m(\xi)) [G_2(u_m(\xi)) + G_3(u_m(\xi))]}]. \quad (5.7)$$

The function $f(\xi)$ describes one of the two boundaries of the
 576 range of fractions m/n that correspond to the vortex knots
 577 $K_{m,n}$ realized for the fluid flow (1.2) defined by the stream
 578 function $\psi(r, z)$ [Eq. (4.7)] for the given ξ .
 579

Equation (4.12) for $\xi = \bar{\xi}_1 \approx 0.11182$ has the root
 580 $u_m(\bar{\xi}_1) = v_1 \approx 4.2329 < \bar{u}_1(0) = \bar{u}_1 \approx 4.4931$. Hence we
 581


 FIG. 3. Plot of the function $f(\xi)$.

and (4.4) has the form

$$\begin{aligned} & [G_1(u) + 3G_2(u)][G_3^2(u) - G_2(u)G_4(u)] \\ & = [G_2(u) + G_3(u)][G_2^2(u) - G_1(u)G_3(u)], \end{aligned}$$

where $u = u_m(\xi)$. The latter equation has the root $\xi_0 \approx 0.1085$; the corresponding value $f(\xi_0) \approx 0.5079$ is the minimal value of the function $f(\xi)$ on the segment $-1/3 \leq \xi \leq \bar{\xi}_1 \approx 0.11182$.

Substituting numerical values $\xi_1 \approx 0.02872$ and $u_m(\xi_1) = u_* \approx 2.9570$ into (5.7), we find $f(\xi_1) \approx 0.7502$, which is the minimal value of the function $f(\xi)$ on the segment I^* : $-1/3 \leq \xi \leq \xi_1 \approx 0.02872$ (see Fig. 3). Substituting the value $u_m(0) = \bar{v}_1 \approx 2.7437$ into formula (5.7), we get $f(0) \approx 0.82524$. The corresponding value of $p(\psi_m)$ is $p(\psi_m) = 2\pi f(0) \approx 5.1849$.

VI. LIMIT OF THE PITCH FUNCTION $p(\psi)$ AT $\psi \rightarrow 0$

All trajectories of the system (4.9) inside the domain D_1 for $-1/3 < \xi \leq \xi_1$ are closed curves C_ψ , $\psi(r, z) = \psi = \text{const}$, $0 < \psi < \psi_m$, encircling the center equilibrium point a_3 and having periods $t(\psi)$. The corresponding trajectories of the system (4.9) and (4.10) are helices moving on invariant tori $\mathbb{T}_\psi^2 = C_\psi \times \mathbb{S}^1 \subset \mathbb{R}^3$ (the circle \mathbb{S}^1 corresponds to the angle φ). In view of (4.10), the pitch $p(\psi)$ of the helices is

$$p(\psi) = \int_0^{t(\psi)} \frac{d\varphi}{dt} dt = -\alpha^2 B \int_0^{t(\psi)} G_2(\alpha R(t)) dt. \quad (6.1)$$

For $\xi \in I^*$, the closed trajectories C_ψ at $\psi \rightarrow 0$ approach the cycle of two separatrices I_1 and S_1 that satisfy the equation $\psi(r, z) = 0$ (see Fig. 2). Since the dynamics along each separatrix takes an infinite time [20] we get

$$\lim_{\psi \rightarrow 0} t(\psi) = \infty. \quad (6.2)$$

At the saddle equilibrium points a_1 and a_2 we have $G_2(a_i) = \xi$. Let $\mathcal{O}_\varepsilon(a_1)$ and $\mathcal{O}_\varepsilon(a_2)$ be small neighborhoods of the points a_1 and a_2 such that inside them $|G_2(\alpha R) - \xi| < \varepsilon$. The velocity \mathbf{v} of the dynamics of any trajectory C_ψ outside $\mathcal{O}_\varepsilon = \mathcal{O}_\varepsilon(a_1) \cup \mathcal{O}_\varepsilon(a_2)$ satisfies $|\mathbf{v}| > \text{const} > 0$. Hence any trajectory C_ψ spends, during one period $t(\psi)$, only a limited time $t_{\text{out}}(\psi) < C \ll t(\psi)$ outside \mathcal{O}_ε and time $t_{\text{in}}(\psi)$ inside \mathcal{O}_ε . In view of (6.2) we have $t_{\text{in}}(\psi) = [t(\psi) - t_{\text{out}}(\psi)] \rightarrow \infty$ at $\psi \rightarrow 0$ and $t_{\text{out}}(\psi) < \text{const}$. Therefore, using (6.1) with $B > 0$ and $G_2(\alpha R) \approx \xi$ in \mathcal{O}_ε we get

$$\lim_{\psi \rightarrow 0} p(\psi) = \begin{cases} +\infty & \text{for } -1/3 < \xi < 0 \\ -\infty & \text{for } 0 < \xi \leq \xi_1. \end{cases} \quad (6.3)$$

For $-1/3 < \xi < 0$ the function $p(\psi)$ monotonically decreases from its limit $p(0) = +\infty$ at $\psi = 0$ to its positive limit value $p(\psi_m) = 2\pi f(\xi)$ [Eq. (5.6)] at $\psi = \psi_m$ (see Fig. 4). Hence all vortex knots for the fluid flow (1.2) with a given ξ ($-1/3 < \xi < 0$) are torus knots $K_{m,n}$ for which the rational numbers m/n are not arbitrary and satisfy the inequalities

$$f(\xi) < \frac{m}{n} < +\infty. \quad (6.4)$$

For $0 < \xi \leq \xi_1$, the function $p(\psi)$ monotonically increases in view of (6.3) from its limit $p(0) = -\infty$ at $\psi = 0$ to its positive limit value (5.6) at $\psi = \psi_m$ (see Fig. 5). Hence, for the fluid flow (1.2) with $0 < \xi \leq \xi_1$ all vortex knots are torus

get $G_2(u_m(\bar{\xi}_1)) = G_2(v_1) < 0$. Numerical calculation gives $G_2(v_1) \approx -0.0140$. Since $u_m(\xi)$ is a monotonically increasing function of $\xi \in [-1/3, \bar{\xi}_1 \approx 0.11182]$ [see the plot of the function $y_2(u)$ in Fig. 1] and $G_2(u)$ is a monotonically increasing function of $u \in [0, u_1 \approx 5.7635]$, we find that $G_2(u_m(\xi))$ is a monotonically increasing function of $\xi \in [-1/3, \bar{\xi}_1]$. Hence, from $G_2(u_m(\bar{\xi}_1)) = G_2(v_1) \approx -0.0140 < 0$ it follows that for all $\xi \in [-1/3, \bar{\xi}_1]$ we have $G_2(u_m(\xi)) < 0$. Hence formulas (5.6) and (5.7) give $p(\psi_m) > 0$ and $f(\xi) > 0$ for all $\xi \in [-1/3, \bar{\xi}_1 \approx 0.11182]$.

In view of the formulas (4.4) we get that Eq. (4.12) near $\xi = -1/3$ is $u_m^2(\xi) \approx 15(\xi + 1/3)$ and $u_m(-1/3) = 0$. From (4.5) we find

$$G_2(0) = -1/3, \quad G_2(0) + G_3(0) = -4/15, \quad G_3(0) = 1/15.$$

Hence we get from (5.7) the asymptotic formula

$$f(\xi) \approx \frac{\sqrt{5/3}}{2\sqrt{\xi + 1/3}} \approx \frac{0.6455}{\sqrt{\xi + 1/3}}, \quad \xi \rightarrow -1/3. \quad (5.8)$$

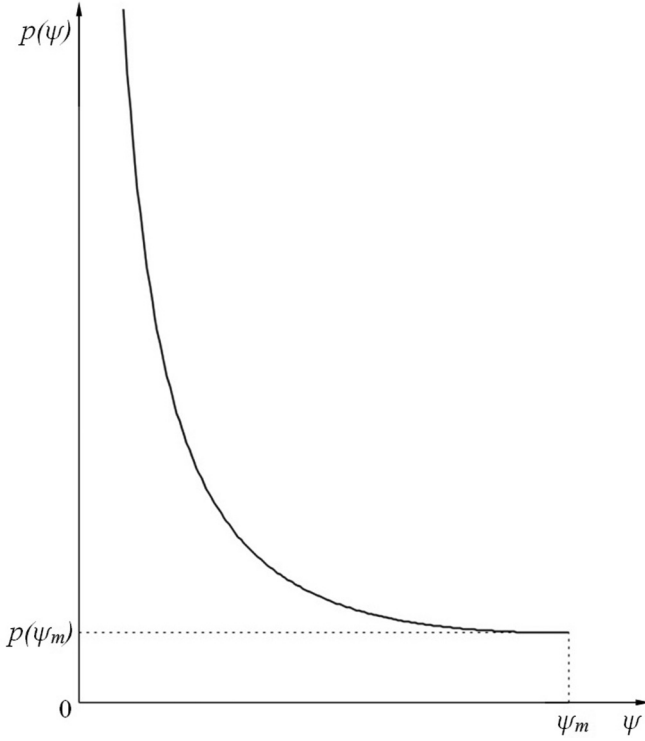
Hence $f(\xi) \rightarrow \infty$ at $\xi \rightarrow -1/3$.

The point $u_m(\bar{\xi}_1) = v_1$ is the point of maximum of the function $-[G_1(u) + G_2(u)]/2$ (see Fig. 1). Hence, using Taylor's formula we get that Eq. (4.12) near $\bar{\xi}_1$ takes the form $\bar{\xi}_1 - \xi \approx \frac{1}{4}v_1^2[G_3(v_1) + G_4(v_1)][u_m(\xi) - v_1]^2$. We have from (4.4) $G_2(v_1) + G_3(v_1) = v_1^{-1}[G_1'(v_1) + G_2'(v_1)] = 0$. Therefore, for $u_m(\xi) \approx v_1$ we have $G_2(u_m(\xi)) + G_3(u_m(\xi)) \approx v_1[G_3(v_1) + G_4(v_1)][u_m(\xi) - v_1]$. Substituting this into (5.7), we find the asymptotes

$$f(\xi) \approx -\frac{G_2(v_1)}{v_1\sqrt{2G_3(v_1)[G_3(v_1) + G_4(v_1)]^{1/4}(\bar{\xi}_1 - \xi)^{1/4}}, \quad \xi \rightarrow \bar{\xi}_1. \quad (5.9)$$

Substituting $v_1 \approx 4.2329$, $G_2(v_1) = -G_3(v_1) \approx -0.0140$, and $G_4(v_1) \approx -0.0031$ into (5.9), we find $f(\xi) \approx 0.0612(\bar{\xi}_1 - \xi)^{-1/4} \rightarrow \infty$ at $\xi \rightarrow \bar{\xi}_1$. The plot of the function $f(\xi)$ is shown in Fig. 3.

To find the minimum of the function $f(\xi)$ we consider the equation $df(\xi)/d\xi = 0$. The equation in view of (5.7)

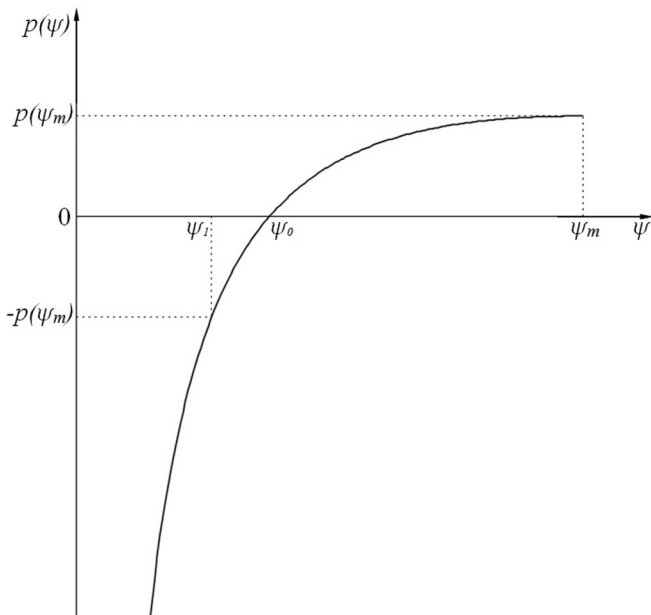
FIG. 4. Plot of the pitch function $p(\psi)$ for $-1/3 < \xi < 0$.

654 knots $K_{|m|,n}$ (where the integer m can be negative) with the
655 ratio m/n satisfying the inequalities

$$-\infty < \frac{m}{n} < f(\xi). \quad (6.5)$$

656

657 In Sec. V we proved that $p(\psi_m) = 2\pi f(\xi) > 0$ for all ξ (see
658 Fig. 3). Hence the function $p(\psi)$ vanishes at some point ψ_0 :
659 $p(\psi_0) = 0$. At some point $\psi_1 < \psi_0$ we have $p(\psi_1) = -p(\psi_m)$

FIG. 5. Plot of the pitch function $p(\psi)$ for $0 < \xi \leq \xi_1$.

(see Fig. 5). For $\psi = \psi_0$ all trajectories of the dynamical
660 system (4.9) and (4.10) on the torus $\mathbb{T}_{\psi_0}^2$ are closed curves
661 that are embedded into \mathbb{R}^3 as unknots because $p(\psi_0) = 0$.
662 All torus knots $K_{m,n}$ for $0 < m/n < f(\xi)$ are realized on two
663 different tori \mathbb{T}_{ψ}^2 : one for ψ in the interval (ψ_0, ψ_m) , where
664 $p(\psi) = 2\pi m/n > 0$, and another one on torus $\mathbb{T}_{\tilde{\psi}}^2$ for $\tilde{\psi}$
665 in the interval (ψ_1, ψ_0) , where $p(\tilde{\psi}) = -2\pi m/n < 0$. The torus
666 knots $K_{m,n}$ corresponding to $p(\psi) = 2\pi m/n > 0$ and $p(\tilde{\psi}) =$
667 $-2\pi m/n < 0$ are nonisotopic mirror images of each other.
668

For the special case $\xi = \lambda = 0$ the vector field \mathbf{V} [Eq. (1.2)]
669 satisfies the Beltrami equation $\text{curl } \mathbf{V} = \alpha \mathbf{V}$ and the analo-
670 gous magnetic field \mathbf{B} is force-free. This is the well-known
671 spheromak equilibrium solution derived by Woltjer [16] and
672 Chandrasekhar [23] and later studied in [25–30]. The term
673 “spheromak” was first introduced in [25]. For $\xi = 0$, the
674 parameter $\bar{u}_1(0) = \bar{u}_1$, where $\bar{u}_1 \approx 4.4931$ is the first positive
675 root of the equation $G_2(u) = 0$.
676

The evaluation of the limit of $p(\psi)$ at $\psi \rightarrow 0$ by formula
677 (6.1) for $\xi = 0$ leads to an uncertainty because $G_2(\alpha R) = 0$ at
678 the equilibrium points a_1 and a_2 and on the separatrix S_1 . To
679 resolve this uncertainty we use another method based on the
680 invariance of the pitch function $p(\psi)$ under the rescaling of
681 r, z , and a reparametrization of time t . In the new coordinates
682 $r_1 = |\alpha|r$, $z_1 = |\alpha|z$, and $u = \sqrt{r_1^2 + z_1^2} = |\alpha|R$ the system
683 (4.9) and (4.10) for $\xi = 0$ is transformed into $[\sigma = \pm 1 =$
684 $\text{sgn}(\alpha)]$
685

$$\sigma \dot{r}_1 = \alpha^2 B r_1 z_1 G_3(u), \quad (6.6)$$

$$\sigma \dot{z}_1 = -2\alpha^2 B G_2(u) - \alpha^2 B r_1^2 G_3(u),$$

$$\dot{\varphi} = -\alpha^2 B G_2(u). \quad (6.7)$$

After the change of time $d\tau/dt = -\alpha^2 B G_2(u)$ the system
686 (6.6) and (6.7) turns into a system that does not depend on the
687 parameters α and B :
688

$$\sigma \frac{dr_1}{d\tau} = -r_1 z_1 \frac{G_3(u)}{G_2(u)}, \quad \sigma \frac{dz_1}{d\tau} = 2 + r_1^2 \frac{G_3(u)}{G_2(u)}, \quad \frac{d\varphi}{d\tau} = 1. \quad (6.8)$$

As above, the closed trajectories C_ψ at $\psi \rightarrow 0$ are ap-
689 proximated by the interval I_1 ($r_1 = 0$ and $-\bar{u}_1 < z_1 < \bar{u}_1$)
690 and the arc S_1 ($r_1^2 + z_1^2 = \bar{u}_1^2$ and $r_1 > 0$). The system (6.8)
691 yields, on the interval I_1 , $r_1 = 0$ and $|dz_1/d\tau| = 2$. Hence the
692 dynamics of the trajectory C_ψ along the interval I_1 takes the
693 time $\tau_1(\psi) \approx 2\bar{u}_1/2 = \bar{u}_1$.
694

The dynamics of C_ψ along the arc S_1 takes an infinitesimally
695 small time $\tau_2(\psi)$. Indeed, since $G_3(\bar{u}_1) = (\bar{u}_1^2 \sqrt{1 + \bar{u}_1^2})^{-1} \neq 0$
696 and $G_2(u) \rightarrow 0$ as $u \rightarrow \bar{u}_1$, we get, for the velocity \mathbf{v} of the
697 dynamics near the arc S_1 ($u = \bar{u}_1$), $|\mathbf{v}| \rightarrow \infty$ when $\psi \rightarrow 0$.
698 Hence $\tau_2(\psi) \rightarrow 0$. Therefore, we get, for the pitch function
699 $p(\psi)$ and for the function of periods $\tau(\psi) = \tau_1(\psi) + \tau_2(\psi)$,
700

$$\lim_{\psi \rightarrow 0} p(\psi) = \int_0^{\tau(\psi)} \frac{d\varphi}{d\tau} d\tau = \lim_{\psi \rightarrow 0} \tau(\psi) = \bar{u}_1 \approx 4.4931. \quad (6.9)$$

The stream function $\psi(r, z)$ [Eq. (4.7)] for $\xi = 0$, $B = 1$,
701 and $\alpha = 1$ attains its maximal value $\psi_m \approx 1.0631$ at the point
702 $r_m \approx 2.7437$, $z_m = 0$. Numerical integration of the system
703 (6.8) shows that on the interval $(0, \psi_m)$ the pitch function $p(\psi)$
704

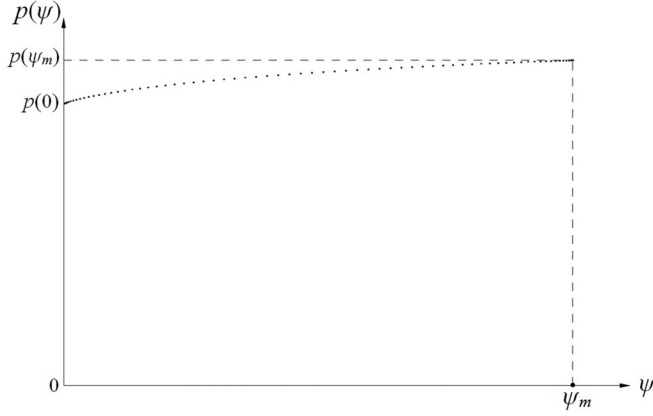


FIG. 6. Numerical calculation of the pitch function $p(\psi)$ for $\xi = 0$.

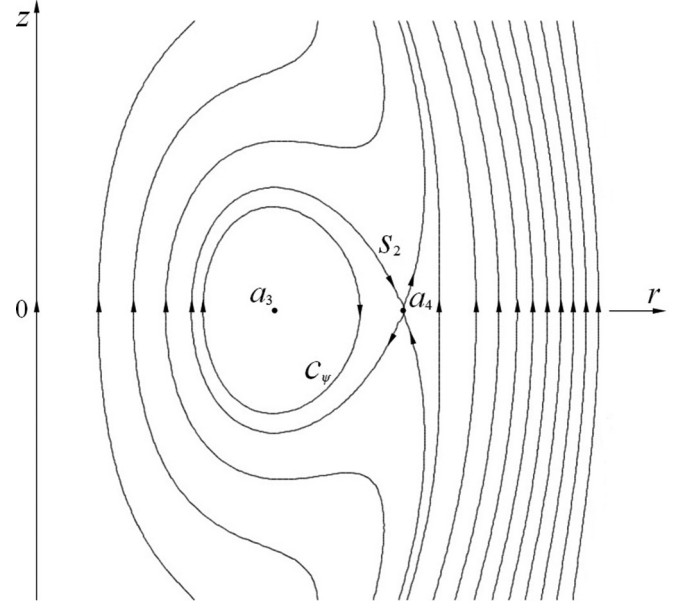


FIG. 7. Poloidal contours of stream surfaces for $\xi = 0.07027$. Rotation of closed contours around the z axis defines the \mathbf{V} -invariant ring \mathcal{R} bounded by the \mathbf{V} -invariant torus $\mathbb{T}^2 = S_2 \times S^1$. Rotation of points a_3 and a_4 gives the stable vortex axis $a_3 \times S^1$ and the unstable one $a_4 \times S^1$. All vortex knots are located inside the ring \mathcal{R} .

705 monotonically increases from its value $p(0) = \bar{u}_1 \approx 4.4931$
 706 [Eq. (6.9)] at $\psi = 0$ to its value $p(\psi_m) = 2\pi f(0) \approx 5.1849$
 707 [Eq. (5.9)] at $\psi = \psi_m$ (see Fig. 6). These results prove that
 708 for the spheromak Beltrami flows corresponding to $\xi = 0$ [or
 709 $\lambda = 0$ in (4.1)] only those torus knots $K_{m,n}$ are realized for
 710 which the fractions m/n satisfy the inequalities

$$\frac{1}{2\pi} 4.4931 \approx 0.7151 < \frac{m}{n} < f(0) \approx 0.8252. \quad (6.10)$$

VII. FLUID FLOWS (1.2) AND (4.7) WITH INVARIANT RINGS

713 For $\xi_1 < \xi < \bar{\xi}_1$, Eq. (4.11) does not have any roots. Hence
 714 the flow (1.2) and (4.7) does not have invariant spheroids \mathbb{B}_c .
 715 Equation (4.12) for the same ξ has two roots $u_m = \alpha r_m$ and
 716 $u_s = \alpha r_s$, $u_m < u_s$ (see Fig. 1). Therefore, the corresponding
 717 dynamical system (4.9) has two equilibrium points: a stable
 718 center a_3 [$(r = r_m, z = 0)$] and an unstable saddle a_4 [$(r =$
 719 $r_s, z = 0)$]. The saddle equilibrium a_4 has a loop separatrix S_2
 720 that begins and ends at the point a_4 and satisfies the equation

$$\psi(r, z) = Br^2[\xi - G_2(\alpha R)] = Br_s^2[\xi - G_2(u_s)] = \psi_s. \quad (7.1)$$

721 The phase portrait of the system (4.9) for $\xi = (\xi_1 + \bar{\xi}_1)/2 \approx$
 722 0.07027 is shown in Fig. 7, where $r_m = 3.37402$ and
 723 $r_s = 5.18961$.

724 The loop separatrix S_2 bounds a domain D_2 that is filled with
 725 closed trajectories C_ψ , which define invariant tori of the dyn-
 726 amical system (4.9) and (4.10), $\mathbb{T}_\psi^2 = C_\psi \times S^1 \subset D_2 \times S^1$.
 727 Here the circle S^1 corresponds to the angular variable φ : $0 \leq$
 728 $\varphi \leq 2\pi$. The closure of the product $D_2 \times S^1$ is an invariant
 729 ring $\mathcal{R}^3 \subset \mathbb{R}^3$.

730 Let us study the structure of the vortex knots inside the ring
 731 \mathcal{R}^3 . The first root of the function $G_2(u)$ [Eq. (4.4)] is $\bar{u}_1 \approx$
 732 4.4931 . Let $\xi_c = -[G_1(\bar{u}_1) + G_2(\bar{u}_1)]/2 \approx 0.1088$. From
 733 Fig. 1 it follows that for $\xi_c < \xi < \bar{\xi}_1$ the roots of Eq. (4.12)
 734 satisfy the inequalities $u_m < u_s < \bar{u}_1$ and hence $G_2(u_s) <$
 735 0 . For $\xi_1 < \xi < \xi_c$ the inequalities are $u_m < \bar{u}_1 < u_s$
 736 and hence $G_2(u_s) > 0$. Using formula (6.1) for the pitch $p(\psi)$
 737 and the fact that the dynamics along the loop separatrix S_2
 738 takes an infinite time, we get (the proof is the same as in

Sec. VI) the following limits of the pitch function $p(\psi)$ for
 trajectories in the domain D_2 at $\psi \rightarrow \psi_s$ [Eq. (7.1)]:

$$\lim_{\psi \rightarrow \psi_s} p(\psi) = \begin{cases} +\infty, & \xi_c < \xi < \bar{\xi}_1 \\ -\infty, & \xi_1 < \xi < \xi_c. \end{cases}$$

741 We proved in Sec. V that near a center equilibrium point of the
 742 system (4.9) at which the function $\psi(r, z)$ has its maximum or
 743 minimum ψ_m the limit of the pitch function $p(\psi)$ at $\psi \rightarrow \psi_m$
 744 is a finite positive number $p(\psi_m) = 2\pi f(\xi)$. Hence we get
 745 that for the vortex knots $K_{m,n}$ realized in the ring \mathcal{R}^3 the ratios
 746 m/n satisfy the inequalities

$$f(\xi) < \frac{m}{n} < +\infty, \quad \xi_c < \xi < \bar{\xi}_1 \quad (7.2)$$

$$-\infty < \frac{m}{n} < f(\xi), \quad \xi_1 < \xi < \xi_c, \quad (7.3)$$

where $f(\xi) \geq f(\xi_0) \approx 0.5079$.

748 The equilibria a_3 and a_4 define, respectively, the stable
 749 and unstable vortex axes of the flow (1.2) and (4.7) in the
 750 invariant ring \mathcal{R}^3 ; both axes are also the exact streamlines
 751 because the tori $\mathbb{T}_\psi^2 = C_\psi \times S^1$ are invariant under both flows
 752 curl $\mathbf{V}(\mathbf{x})$ and $\mathbf{V}(\mathbf{x})$. All trajectories of the system (4.9) outside
 753 the domain D_2 are infinite curves satisfying the equation
 754 $Br^2[\xi - G_2(\alpha R)] = \psi = \text{const}$. Hence, for these trajectories
 755 at $t \rightarrow \pm\infty$ we have $z \rightarrow \pm\infty$ and $r \rightarrow r_\xi = \sqrt{\psi/B\xi}$ (see
 756 Fig. 7).

757 For $\xi > \bar{\xi}_1$ or $\xi < -1/3$ both Eqs. (4.11) and (4.12) have
 758 no solutions (see Fig. 1). Therefore, the dynamical system
 759 (4.9) has no equilibrium points and no closed trajectories.
 760 For all its trajectories at $t \rightarrow \pm\infty$ we have $z \rightarrow \pm\infty$ and
 761 $r \rightarrow r_\xi = \sqrt{\psi/B\xi}$. Hence the fluid flows (1.2) and (4.7) for
 762 $\xi > \bar{\xi}_1$ or $\xi < -1/3$ have no vortex knots.

VIII. LIQUID PLANET MODEL

763

764 The fluid velocity field $\mathbf{V}_\xi(r, z)$ [Eq. (1.20)] for $-1/3 <$
 765 $\xi \leq \xi_1 \approx 0.02872$, $\xi \neq 0$, has a finite number $N(\xi)$ of
 766 invariant spheres $\mathbb{S}_{a_k}^2$ of radii $R = a_k$ satisfying the equation
 767 $G_2(\alpha a_k) = \xi$. On each sphere $\mathbb{S}_{a_k}^2$ the flow takes the form

$$\bar{\mathbf{V}}_\xi(r, z) = \alpha^2 r G_3(\alpha a_k) [z \hat{\mathbf{e}}_r - r \hat{\mathbf{e}}_z] \quad (8.1)$$

768 and is evidently tangent to the sphere $\mathbb{S}_{a_k}^2$. Hence each spheroid
 769 $\mathbb{B}_{a_k}^3$ defined by the inequality $R \leq a_k$ is invariant under the
 770 flow (1.20).

771 The velocity field (8.1) vanishes for the special val-
 772 ues of ξ when $G_3(\alpha a_\ell) = 0$. Since $G_3(u) = u^{-1} dG_2(u)/du$
 773 [Eq. (4.4)], the equation $G_3(u_\ell) = 0$ means that u_ℓ is a point
 774 of extremum of the function $G_2(u)$. Using formula (4.4) we
 775 find that the equation $G_3(u) = 0$ is equivalent to the equation

$$\tan u = \frac{3u}{3 - u^2}. \quad (8.2)$$

776 Hence the roots u_ℓ of the equation $G_3(u) = 0$ or Eq. (8.2) have
 777 the asymptotes $u_\ell \approx (\ell + 1)\pi$ and $u_\ell < (\ell + 1)\pi$ at $\ell \rightarrow \infty$.
 778 The first eight roots of Eq. (8.2) are

$$\begin{aligned} u_1 &\approx 5.7635, & u_2 &\approx 9.0950, & u_3 &\approx 12.3229, \\ u_4 &\approx 15.5146, & u_5 &\approx 18.6890, & u_6 &\approx 21.8539, \\ u_7 &\approx 25.0128, & u_8 &\approx 28.1678. \end{aligned}$$

779 Let us define $\xi_\ell = G_2(u_\ell)$. Substituting $G_3(u_\ell) = 0$ into
 780 the second identity (4.6), we find $\xi_\ell = -G_1(u_\ell)/3 =$
 781 $-(3u_\ell)^{-1} \sin u_\ell$. Formula (8.2) yields $-(3u_\ell)^{-1} \sin u_\ell =$
 782 $\cos u_\ell / (u_\ell^2 - 3)$. Hence we get the exact formula

$$\xi_\ell = \frac{\cos u_\ell}{u_\ell^2 - 3}. \quad (8.3)$$

783 Using $u_\ell \approx (\ell + 1)\pi$, we find from (8.3) the asymptotes
 784 $\xi_\ell \approx (-1)^{\ell+1} (u_\ell)^{-2}$ at $\ell \rightarrow \infty$.

785 The first eight values of $\xi_\ell = G_2(u_\ell)$ [Eq. (8.3)] are

$$\begin{aligned} \xi_1 &\approx G_2(u_1) \approx 0.02872, & \xi_2 &\approx -0.0119, & \xi_3 &\approx 0.0065, \\ \xi_4 &\approx -0.0041, & \xi_5 &\approx 0.0029, & \xi_6 &\approx -0.0021, \\ \xi_7 &\approx 0.0016, & \xi_8 &\approx -0.0013. \end{aligned}$$

786 The positive values $\xi_\ell > 0$ are local maxima of the function
 787 $G_2(u)$ and the negative values $\xi_\ell < 0$ are local minima (see
 788 Fig. 1).

789 For the special values of $\xi = \xi_\ell$ flow (8.1) vanishes on
 790 the sphere $\mathbb{S}_{a_\ell}^2$ of radius $a_\ell = \alpha^{-1} u_\ell$, because $G_3(u_\ell) = 0$.
 791 Therefore, the flow inside the invariant spheroid $\mathbb{B}_{a_\ell}^3$, $R \leq a_\ell$,
 792 can be continuously matched with empty space. Indeed, from
 793 the equilibrium equations (1.6) we find, on the sphere $\mathbb{S}_{a_\ell}^2$,

$$\rho^{-1} p(\mathbf{x}) + \rho \mu \Phi(\mathbf{x}) + |\mathbf{V}_{\xi_\ell}(\mathbf{x})|^2 / 2 = C, \quad (8.4)$$

794 where C is an arbitrary constant. Since the fluid density ρ is
 795 constant by assumption, we get that the Newtonian potential
 796 $\Phi(\mathbf{x})$ is spherically symmetric and therefore $\Phi(\mathbf{x}) = \Phi(a_\ell)$ on
 797 the sphere $|\mathbf{x}| = a_\ell$. Therefore, using the vanishing of velocity
 798 $\mathbf{V}_{\xi_\ell}(r, z)$ [Eq. (8.1)] on the sphere $\mathbb{S}_{a_\ell}^2$ and choosing the arbitrary
 799 constant $C = \rho \mu \Phi(a_\ell)$, we get from (8.4) that pressure $p(\mathbf{x}) = 0$
 800 on the sphere $\mathbb{S}_{a_\ell}^2$. Therefore, all conditions at the boundary
 801 with empty space are satisfied and thus the flow (1.2) for $\xi = \xi_\ell$

802 is correctly matched with empty space outside the invariant
 803 spheroid $\mathbb{B}_{a_\ell}^3$. We propose these exact solutions as a liquid
 804 planet model.

805 The fluid flow $\mathbf{V}_{\xi_1}(r, z)$ [Eq. (1.20)], $\xi_1 = G_2(u_1)$, has no
 806 other invariant spheroids inside the $\mathbb{B}_{a_1}^3$, where $a_1 = \alpha^{-1} u_1$.
 807 For all other flows $\mathbf{V}_{\xi_\ell}(r, z)$ [Eq. (1.20)] there exists at least one
 808 interior invariant spheroid $\mathbb{B}_{a_k}^3 \subset \mathbb{B}_{a_\ell}^3$. The plot of the function
 809 $y_1(u) = G_2(u)$ in Fig. 1 shows that for $\xi_\ell > 0$ the number of in-
 810 terior invariant spheroids is even; for $\xi_\ell < 0$ the number is odd.

811 *Remark 4.* The first invariant sphere $\mathbb{S}_{a_k}^2 \subset \mathbb{B}_{a_\ell}^3$ can be
 812 considered as the interior boundary of the flow, for $\ell > 1$.
 813 In this case the fluid moves with velocity $\mathbf{V}_{\xi_\ell}(r, z)$ [Eq. (1.20)]
 814 in the spherical shell $a_k < R \leq a_\ell$ and the spheroid $\mathbb{B}_{a_k}^3$ (where
 815 $R \leq a_k$) is the rigid core of the planet with a spherically
 816 symmetric distribution of mass. For the ideal fluid model the
 817 no-slip condition at the interior boundary $\mathbb{S}_{a_k}^2$ can be relaxed
 818 because it is necessary only for viscous fluids.

819 The problem of equilibrium of magnetic stars with a
 820 dipole field outside was studied by Chandrasekhar and Fermi
 821 in [31]. The first example of the magnetic field that is
 822 continuously matched with an empty space was derived
 823 by Prendergast under the condition $J_{5/2}(\alpha a) = 0$ [17]. Our
 824 condition $G_3(\alpha a) = 0$ coincides with the Prendergast one in
 825 view of the formula for the Bessel function

$$\begin{aligned} J_{5/2}(u) &= \frac{1}{\sqrt{\pi/2} u^{3/2}} \left[(3 - u^2) \frac{\sin u}{u} - 3 \cos u \right] \\ &= \frac{u^{5/2}}{\sqrt{\pi/2}} G_3(u), \end{aligned}$$

which follows from [24] (p. 56).

IX. CONCLUSION

826 As known [32,33], the torus knots $K_{m,n}$ are nontrivial unless
 827 $m/n = N$ or $m/n = 1/N$, where N is an integer. All other
 828 torus knots are mutually nonisotopic. A torus knot $K_{m,n}$ with
 829 $m/n \neq N, 1/N$ and its mirror image [which corresponds to
 830 the pair $(-m, n)$] are nonisotopic to each other. Therefore, we
 831 obtain from (6.4) that the set of mutually nonisotopic vortex
 832 torus knots $K_{m,n}$ for fluid flows (1.2) and (4.7) inside the
 833 first invariant spheroid \mathbb{B}_{a_1} with the parameter ξ in the range
 834 $-1/3 < \xi < 0$ is equivalent to the set of all rational numbers
 835 m/n satisfying relations
 836 m/n satisfying relations
 837

$$f(\xi) < \frac{m}{n} < +\infty, \quad \frac{m}{n} \neq N, \quad (9.1)$$

838 where N is any integer. Here the lower bound $f(\xi) >$
 839 $f(0) \approx 0.8252$ and $f(\xi) \approx 0.6455(\xi + 1/3)^{-1/2} \rightarrow \infty$ when
 840 $\xi \rightarrow -1/3$ [see (5.8)]. Formula (9.1) implies that all flows
 841 (1.2) and (4.7) for $-1/3 < \xi < 0$ in view of $f(\xi) > 0.8252$ are
 842 counterexamples to the Moffatt statement (see [2], p. 129): “It
 843 is interesting that every torus knot is represented once and only
 844 once among all the vortex lines of each member of the family
 845 of flows represented by the stream function (54), together with
 846 circulation (52)”.

847 From Fig. 3 it follows that for any real number $x > 0.8252$
 848 there exist $\xi(x) \in [-1/3, 0]$ such that $f(\xi(x)) = x$ (see Fig. 3).
 849 For the flow (1.2) and (4.7) with the parameter $\xi = \xi(x)$ only
 850 torus knots $K_{m,n}$ with $m/n > x$ are realized as vortex knots
 851 and all torus knots $K_{\bar{m}, \bar{n}}$ with $\bar{m}/\bar{n} \leq x$ are not realized.

852 If the parameter ξ is in the range $0 < \xi < \xi_1 \approx 0.02872$
 853 then Eq. (6.5) yields that the set of mutually nonisotopic
 854 vortex torus knots $K_{m,n}$ for the flows (1.2) and (4.7) inside the
 855 first invariant spheroid \mathbb{B}_{a_1} is equivalent to the set of rational
 856 numbers m/n defined by the conditions

$$-\infty < \frac{m}{n} < f(\xi), \quad \frac{m}{n} \neq \pm N, \quad \frac{m}{n} \neq \pm \frac{1}{N}, \quad (9.2)$$

857 where N is any integer and $f(0) \approx 0.8252 > f(\xi) > f(\xi_1) \approx$
 858 0.7502 . Note that torus knots $K_{|m|,|n|}$ with $|m|/|n| < f(\xi)$
 859 appear as vortex knots twice: For the positive rational numbers
 860 m/n satisfying $0 < m/n < f(\xi)$ and for the negative ones
 861 satisfying $-f(\xi) < -m/n < 0$, the corresponding knots $K_{m,n}$
 862 and $K_{-m,n}$ are nonisotopic mirror images of each other.
 863 These results also are counterexamples to the above Moffatt
 864 statement. Indeed, here we have torus knots $K_{|m|,|n|}$ realized
 865 on infinitely many pairs of different tori \mathbb{T}_ψ^2 and $\mathbb{T}_{\tilde{\psi}}^2$ on that the
 866 pitch function $p(\psi) = -p(\tilde{\psi})$, so realized *twice* and not “once
 867 and only once” as it is claimed in [2]. Note that the existence
 868 of the pitch functions $p(\psi)$ changing their sign on the segment
 869 $0 \leq \psi \leq \psi_m$ (as in Fig. 5) was never discussed in [2–4].

870 For $\xi = 0$ the fluid flow (1.2) and (4.7) coincides with the
 871 spheromak Beltrami field [16,23,25]. From Eq. (6.10) we get
 872 that the set of mutually nonisotopic vortex torus knots $K_{m,n}$
 873 inside the first invariant spheroid \mathbb{B}_{a_1} is equivalent to the set of
 874 all rational numbers m/n satisfying the inequalities

$$0.7151 < \frac{m}{n} < f(0) \approx 0.8252. \quad (9.3)$$

875 This result is a counterexample to the Moffatt statement in [3]
 876 (pp. 30–31): “It is an intriguing property of this \mathbf{B} -field that
 877 if we take a subset of the \mathbf{B} -lines consisting of one \mathbf{B} -line on
 878 each toroidal surface, then every torus knot is represented once
 879 and only once in this subset, since $p/2\pi$ passes through every
 880 rational number m/n once as it decreases continuously from
 881 infinity to zero”.

882 Note that here the magnetic field \mathbf{B} knots are discussed,
 883 but since the considered field satisfies the Beltrami equation
 884 $\text{curl } \mathbf{B} = \alpha \mathbf{B}$, the \mathbf{B} lines coincide with the $\text{curl } \mathbf{B}$ lines.
 885 Therefore, the above statement of [3] is applicable also to the
 886 vortex knots of the steady fluid flow with $\mathbf{V}(\mathbf{x}) \equiv \mathbf{B}(\mathbf{x})$
 887 [Eqs. (1.2) and (4.7)] with $\xi = 0$ (and also is incorrect).

888 Since the function $f(\xi)$ [Eq. (5.7)] for $-1/3 < \xi < \xi_1$ is
 889 monotonically decreasing (see Fig. 3), we get that all families
 890 of nonisotopic vortex torus knots $K_{m,n}$ [Eqs. (9.1)–(9.3)] are

891 different for flows (1.2) and (4.7) with different values of the
 892 parameter ξ . Among these families of vortex knots in view of
 893 $f(\xi) \geq 0.5079$ for all ξ no one family coincides with Moffatt’s
 894 description in [2,3]. Therefore, Moffatt’s statements of [2,3]
 895 on vortex knots do not correspond to the facts.

896 For any axisymmetric steady fluid flows [defined by
 897 arbitrary smooth functions $H(\psi)$ and $C(\psi)$ in Eq. (1.3)] for
 898 which the function $\psi(r, z)$ has a nondegenerate maximum or
 899 minimum ψ_m at a point $a_m(r_m, z_m)$, we have proved in Sec. II
 900 that the pitch function $p(\psi)$ has a finite and nonzero limit at
 901 $\psi \rightarrow \psi_m$:

$$p(\psi_m) = \lim_{\psi \rightarrow \psi_m} p(\psi) = \frac{2\pi r_m}{|C'(\psi_m)|\sqrt{\mathcal{H}(a_m)}} \left[-H'(\psi_m) + \frac{1}{r_m^2} C(\psi_m)C'(\psi_m) \right]. \quad (9.4)$$

902 Formula (9.4) demonstrates that presented in [2,3] Moffatt’s
 903 statements that for the special flows (1.2) and (4.1)
 904 $\lim_{\psi \rightarrow \psi_{\max}} p(\psi) = \infty$ are incorrect because for these flows
 905 $C'(\psi_m) = \alpha \neq 0$ and $\mathcal{H}(a_m) \neq 0$.

906 Formula (9.4) yields a plethora of counterexamples to the
 907 concluding part of Moffatt’s statement of [4] (p. 29): “The
 908 streamlines within these vortices are topologically similar to
 909 those of the special case when $F(\psi)$ and $G(\psi)$ are linear in
 910 ψ , [i.e.,] they are helices wrapped on the family of nested tori
 911 [$\psi = \text{const}(0 < \psi < \psi_{\max})$], the pitch of the helix varying
 912 continuously from zero . . . to infinity . . .”. Indeed, for the
 913 generic functions $F(\psi)$ and $G(\psi)$ [or $H(\psi)$ and $C(\psi)$ in (1.3)]
 914 the limit value $p(\psi_m)$ [Eq. (9.4)] evidently is nonzero and is
 915 one of the two exact bounds for the range of the function $p(\psi)$.
 916 Since the bound $p(\psi_m) \neq 0$ we get that the pitch function $p(\psi)$
 917 does not change “continuously from zero to infinity”.

918 For some functions $H(\psi)$ and $C(\psi)$ the stream function
 919 $\psi(r, z)$ satisfying Eq. (1.3) can have no maxima or minima at
 920 all. Then the fluid flow (1.2) does not have invariant tori \mathbb{T}_ψ^2 ,
 921 vortex knots, or pitch function $p(\psi)$. This is realized for the
 922 exact fluid flows (1.2) and (4.7), with the parameter $\xi < -1/3$
 923 or $\xi > \xi_1 \approx 0.11182$, and for some exact solutions to the
 924 Grad-Shafranov equation (1.3) derived in [13,14].

ACKNOWLEDGMENT

925 The author thanks the referees for useful remarks. 926

[1] G. Batchelor, *An Introduction to Fluid Dynamics* (Cambridge University Press, Cambridge, 1967).
 [2] H. K. Moffatt, The degree of knottedness of tangled vortex lines, *J. Fluid Mech.* **35**, 117 (1969).
 [3] H. K. Moffatt, *Magnetic Field Generation in Electrically Conducting Fluids* (Cambridge University Press, Cambridge, 1978).
 [4] H. K. Moffatt, *Proceedings of the IUTAM Symposium on Fundamental Aspects of Vortex Motion, Tokyo, 1987* (North-Holland, Amsterdam, 1988), pp. 22–30.
 [5] S. Chandrasekhar and K. Prendergast, The equilibrium of magnetic stars, *Proc. Natl. Acad. Sci. USA* **42**, 5 (1956).

[6] M. Kruskal and R. Kulsrud, Equilibrium of a magnetically confined plasma in a toroid, *Phys. Fluids* **1**, 265 (1958).
 [7] P. Alexandroff and H. Hopf, *Topology* (Springer, Berlin, 1935), p. 552.
 [8] W. Newcomb, Magnetic differential equations, *Phys. Fluids*, **2**, 362 (1959).
 [9] C. Mercier, Equilibre et satabilite d’un systeme toroidal magneto-hydrodynamique au voisinage d’un axe magnetique, *Fusion Nucl.* **4**, 213 (1964).
 [10] V. Arnold, Sur la topologie des ecoulements stationnaires des fluides parfaits, *C. R. Acad. Sci. Paris* **261**, 17 (1965).
 [11] V. I. Arnold, On the topology of three-dimensional steady flows of an ideal fluid, *J. Appl. Math. Mech.* **30**, 223 (1966).

- [12] J. P. Freidberg, *Plasma Physics and Fusion Energy* (Cambridge University Press, Cambridge, 2007).
- [13] O. I. Bogoyavlenskij, Astrophysical Jets as Exact Plasma Equilibria, *Phys. Rev. Lett.* **84**, 1914 (2000).
- [14] O. I. Bogoyavlenskij, Counterexamples to Parker's theorem, *J. Math. Phys.* **41**, 2043 (2000).
- [15] O. I. Bogoyavlenskij, Helically symmetric astrophysical jets, *Phys. Rev. E* **62**, 8616 (2000).
- [16] L. Woltjer, The Crab Nebula, *Bull. Astron. Inst. Neth.* **14**, 39 (1958).
- [17] K. Prendergast, The equilibrium of a self-gravitating incompressible fluid sphere with a magnetic field. I., *Astrophys. J.* **123**, 498 (1957).
- [18] O. Bogoyavlenskij, Moduli spaces of vortex knots for an exact fluid flow, *J. Math. Phys.* **58**, 013101 (2017).
- [19] O. Bogoyavlenskij, Vortex knots for the spheromak fluid flow and their moduli spaces, *J. Math. Anal. Appl.* **450**, 21 (2017).
- [20] E. Ince, *Ordinary Differential Equations* (Dover, New York, 1956).
- [21] W. Newcomb, Motion of magnetic lines of force, *Ann. Phys. (NY)* **3**, 347 (1958).
- [22] P. Bellan, *Fundamentals of Plasma Physics* (Cambridge University Press, Cambridge, 2008).
- [23] S. Chandrasekhar, On force-free magnetic fields, *Proc. Natl. Acad. Sci. USA* **42**, 1 (1956).
- [24] G. Watson, *A Treatise on the Theory of Bessel Functions* (Cambridge University Press, Cambridge, 1980).
- [25] M. Rosenbluth and M. Bussac, MHD stability of spheromak, *Nucl. Fusion* **19**, 489 (1979).
- [26] Z. Yoshida and Y. Giga, Remarks on spectra of operator rot, *Math. Zeitschrift* **204**, 235 (1990).
- [27] G. F. Torres del Castillo, Eigenfunctions of the curl operator in spherical coordinates, *J. Math. Phys.* **35**, 499 (1994).
- [28] G. E. Marsh, *Force-free Magnetic Fields: Solutions, Topology and Applications* (World Scientific, Singapore, 1996).
- [29] J. Cantarella, D. DeTurck, H. Gluck, and M. Teytel, The spectrum of the curl operator on spherically symmetric domains, *Phys. Plasmas* **7**, 2766 (2000).
- [30] E. Morse, Eigenfunctions of the curl in cylindrical geometry, *J. Math. Phys.* **46**, 113511 (2005).
- [31] S. Chandrasekhar and F. Fermi, Problems of gravitational stability in the presence of a magnetic field, *Astrophys. J.* **118**, 116 (1953).
- [32] R. Crowell and R. Fox, *Introduction to Knot Theory* (Ginn, Boston, 1963).
- [33] D. Rolfsen, *Knots and Links* (Publish or Perish, Houston, 1990).